NOAA Technical Memorandum NWS WR-207

THE LAS VEGAS McCARRAN INTERNATIONAL AIRPORT MICROBURST OF AUGUST 8, 1989

Carven A. Scott

Weather Service Nuclear Support Office
Las Vegas, Nevada
June 1990

NOAA TECHNICAL MEMORANDA
National Weather Service, Western Region Subseries

The National Weather Service (NWS) Western Region (WR) Subseries provides an informal medium for the documentation and quick dissemination of results not appropriate, or not yet ready, for formal publication. The series is used to report on work in progress, to describe technical procedures and practices, or to relate progress to a limited audience. These Technical Memoranda will report on investigations devoted primarily to regional and local problems of interest mainly to personnel, and hence will not be widely distributed.

Papers 1 to 25 are in the former series, ESSA Technical Memoranda, Western Region Technical Memoranda (WRTM); papers 24 to 59 are in the former series, ESSA Technical Memoranda, Weather Bureau Technical Memoranda (WBTM). Beginning with 60, the papers are part of the series, NOAA Technical Memoranda NWS. Out-of-print memoranda are not listed.

Papers 2 to 22, except for 5 (revised edition), are available from the National Weather Service Western Region, Scientific Services Division, P.O. Box 11188, Federal Building, 125 South State Street, Salt Lake City, Utah 84147. Paper 5 (revised edition), and all others beginning with 25 are available from the National Technical Information Service, U.S. Department of Commerce, Sills Building, 5285 Port Royal Road, Springfield, Virginia 22161. Prices vary for all paper copies; microfiche are $3.50. Order by accession number shown in parentheses at end of each entry.

ESSA Technical Memoranda (WRTM)

2 Climatological Precipitation Probabilities. Compiled by Lucianne Miller, December 1965.
3 Western Region Pre- and Post-FP-3 Program, December 1, 1965, to February 20, 1966. Edward D. Diemer, March 1966.
5 Station Descriptions of Local Effects on Synoptic Weather Patterns. Philip Williams, Jr., April 1966 (Revised November 1967, October 1969). (PB-17800)
8 Interpreting the RAREP. Herbert P. Benner, May 1966 (Revised January 1967).
11 Some Electrical Processes in the Atmosphere. J. Latham, June 1966.
17 A Digitalized Summary of Radar Echoes within 100 Miles of Sacramento, California. J. A. Youngberg and L. B. Overaas, December 1966.
21 An Objective Aid for Forecasting the End of East Winds in the Columbia Gorge, July through October. D. John Coparanis, April 1967.
22 Derivation of Radar Horizons in Mountainous Terrain. Roger G. Pappas, April 1967.

ESSA Technical Memoranda, Weather Bureau Technical Memoranda (WBTM)

25 Verification of Operation Probability of Precipitation Forecasts, April 1966-March 1967. W. W. Dickey, October 1967. (PB-176240)
26 A Study of Winds in the Lake Mead Recreation Area. R. P. Augulis, January 1968. (PB-177830)
28 Weather Extremes. R. J. Schmidli, April 1968 (Revised March 1986). (PB86 177672/AS)
29 Small-Scale Analysis and Prediction. Philip Williams, Jr., May 1968. (PB178425)
30 Numerical Weather Prediction and Synoptic Meteorology. CPT Thomas D. Murphy, USAF, May 1968. (AD 673365)
31 Precipitation Detection Probabilities by Salt Lake ARTC Radars. Robert K. Belesky, July 1968. (PB 179084)
32 Probability Forecasting--A Problem Analysis with Reference to the Portland Fire Weather District. Harold S. Ayer, July 1968. (PB 179289)

36 Temperature Trends in Sacramento--Another Heat Island. Anthony D. Lentini, February 1969. (PB 183055)
37 Disposal of Logging Residues Without Damage to Air Quality. Owen P. Cramer, March 1969. (PB 183057)
39 Upper-Air Lows Over Northwestern United States. A.L. Jacobson, April 1969. PB 184296)
40 The Man-Machine Mix in Applied Weather Forecasting in the 1970s. L.W. Snellman, August 1969. (PB 185068)
43 Forecasting Maximum Temperatures at Helena, Montana. David E. Olsen, October 1969. (PB 185762)
44 Estimated Return Periods for Short-Duration Precipitation in Arizona. Paul C. Kangieser, October 1969. (PB 187763)
46 Applications of the Net Radiometer to Short-Range Fog and Stratus Forecasting at Eugene, Oregon. L. Yee and E. Bates, December 1969. (PB 190476)
47 Statistical Analysis as a Flood Routing Tool. Robert J.C. Burnash, December 1969. (PB 188744)
48 Tsunami. Richard P. Augulis, February 1970. (PB 190157)
49 Predicting Precipitation Type. Robert J.C. Burnash and Floyd E. Hug, March 1970. (PB 190962)
50 Statistical Report on Aerocallergens (Pollens and Molds) Fort Huachuca, Arizona, 1969. Wayne S. Johnson, April 1970. (PB 191743)
51 Western Region Sea State and Surf Forecaster's Manual. Gordon C. Shields and Gerald B. Burdwell, July 1970. (PB 193102)
52 Sacramento Weather Radar Climatology. R.G. Pappas and C. M. Veliquette, July 1970. (PB 193347)
54 A Refinement of the Vorticity Field to Delineate Areas of Significant Precipitation. Barry B. Aronovitch, August 1970.
55 Application of the SSARR Model to a Basin without Discharge Record. Vail Schermerhorn and Donal W. Kuehl, August 1970. (PB 194394)
56 Areal Coverage of Precipitation in Northwestern Utah. Philip Williams, Jr., and Werner J. Heck, September 1970. (PB 194389)
57 Preliminary Report on Agricultural Field Burning vs. Atmospheric Visibility in the Willamette Valley of Oregon. Earl M. Bates and David O. Chilcote, September 1970. (PB 194710)
58 Air Pollution by Jet Aircraft at Seattle-Tacoma Airport. Wallace R. Donaldson, October 1970. (COM 71 00017)
59 Application of PE Model Forecast Parameters to Local-Area Forecasting. Leonard W. Snellman, October 1970. (COM 71 00016)
60 An Aid for Forecasting the Minimum Temperature at Medford, Oregon, Arthur W. Fritz, October 1970. (COM 71 00120)
63 700-mb Warm Air Advection as a Forecasting Tool for Montana and Northern Idaho. Norris E. Woerner, February 1971. (COM 71 00349)
64 Wind and Weather Regimes at Great Falls, Montana. Warren B. Price, March 1971.
65 Climate of Sacramento, California. Tony Martini, April 1990. (Fifth Revision) (PB89 207781/AS)
66 A Preliminary Report on Correlation of ARTCC Radar Echoes and Precipitation. Wilbur K. Hall, June 1971. (COM 71 00829)
69 National Weather Service Support to Soaring Activities. Ellis Burton, August 1971. (COM 71 00956)
71 Western Region Synoptic Analysis-Problems and Methods. Philip Williams, Jr., February 1972. (COM 72 10433)
74 Thunderstorms and Hail Days Probabilities in Nevada. Clarence M. Sakamoto, April 1972. (COM 72 10554)
75 A Study of the Low Level Jet Stream of the San Joaquin Valley. Ronald A. Willis and Philip Williams, Jr., May 1972. (COM 72 10707)
76 Monthly Climatological Charts of the Behavior of Fog and Low Stratus at Los Angeles International Airport. Donald M. Gales, July 1972. (COM 72 11140)
77 A Study of Radar Echo Distribution in Arizona During July and August. John E. Hales, Jr., July 1972. (COM 72 11136)
78 Forecasting Precipitation at Bakersfield, California, Using Pressure Gradient Vectors. Earl T. Riddiough, July 1972. (COM 72 11146)
79 Climate of Stockton, California. Robert C. Nelson, July 1972. (COM 72 10920)
80 Estimation of Number of Days Above or Below Selected Temperatures. Clarence M. Sakamoto, October 1972. (COM 72 10021)
81 An Aid for Forecasting Summer Maximum Temperatures at Seattle, Washington. Edgar G. Johnson, November 1972. (COM 73 10150)
82 Flash Flood Forecasting and Warning Program in the Western Region. Philip Williams, Jr., Chester L. Glenn, and Roland L. Raetz, December 1972, (Revised March 1978). (COM 73 10251)
83 A comparison of Manual and Semiautomatic Methods of Digitizing Analog Wind Records. Glenn E. Rasch, March 1973. (COM 73 10669)
86 Conditional Probabilities for Sequences of Wet Days at Phoenix, Arizona. Paul C. Kangieser, June 1973. (COM 73 11264)
87 A Refinement of the Use of K-Values in Forecasting Thunderstorms in Washington and Oregon. Robert Y.G. Lee, June 1973. (COM 73 11276)
89 Objective Forecast Precipitation Over the Western Region of the United States. Julia N. Paegle and Larry P. Kierulff, September 1973. (COM 73 11946/3AS)
91 Arizona "Eddy" Tornadoes. Robert S. Ingram, October 1973. (COM 73 10465)
92 Smoke Management in the Willamette Valley. Earl M. Bates, May 1974. (COM 74 11277/AS)
93 An Operational Evaluation of 500-mb Type Regression Equations. Alexander E. MacDonald, June 1974. (COM 74 11407/AS)
94 Conditional Probability of Visibility Less than One-Half Mile in Radiation Fog at Fresno, California. John D. Thomas, August 1974. (COM 74 11555/AS)
95 Climate of Flagstaff, Arizona. Paul W. Sorenson, and updated by Reginald W. Preston, January 1987. (PB87 143160/AS)
96 Map type Precipitation Probabilities for the Western Region. Glenn E. Rasch and Alexander E. MacDonald, February 1975. (COM 75 10428/AS)
97 Eastern Pacific Cut-Off Low of April 21-28, 1974. William J. Alder and George R. Miller, January 1976. (PB 250 711/AS)
98 Study on a Significant Precipitation Episode in Western United States. Ira S. Brenner, April 1976. (COM 75 10719/AS)
99 A Study of Flash Flood Susceptibility-A Basin in Southern Arizona. Gerald Williams, August 1975. (COM 75 11360/AS)
102 A Set of Rules for Forecasting Temperatures in Napa and Sonoma Counties. Wesley L. Tuft, October 1975. (PB 246 902/AS)
103 Application of the National Weather Service Flash-Flood Program in the Western Region. Gerald Williams, January 1976. (PB 253 053/AS)
104 Objective Aids for Forecasting Minimum Temperatures at Reno, Nevada, During the Summer Months. Christopher D. Hill, January 1976. (PB 252 866/AS)
105 Forecasting the Mono Wind. Charles P. Ruscha, Jr., February 1976. (PB 254 650)
106 Use of MOS Forecast Parameters in Temperature Forecasting. John C. Plankinton, Jr., March 1976. (PB 254 649)
107 Map Types as Aids in Using MOS PoPs in Western United States. Ira S. Brenner, August 1976. (PB 259 594)
108 Other Kinds of Wind Shear. Christopher D. Hill, August 1976. (PB 260 437/AS)

109 Forecasting North Winds in the Upper Sacramento Valley and Adjoining Forests. Christopher E. Fontana, September 1976. (PB 273 677/AS)
110 Cool Inflow as a Weakening Influence on Eastern Pacific Tropical Cyclones. William J. Denney, November 1976. (PB 264 655/AS)
112 The MAN/MOS Program. Alexander E. MacDonald, February 1977. (PB 265 941/AS)
113 Winter Season Minimum Temperature Formula for Bakersfield, California, Using Multiple Regression. Michael J. Oard, February 1977. (PB 273 694/AS)
114 Tropical Cyclone Kathleen. James R. Fors, February 1977. (PB 273 676/AS)
116 A Study of Wind Gusts on Lake Mead. Bradley Colman, April 1977. (PB 268 847)
117 The Relative Frequency of Cumulonimbus Clouds at the Nevada Test Site as a Function of K-Value. R.F. Quiring, April 1977. (PB 272 831)
118 Moisture Distribution Modification by Upward Vertical Motion. Ira S. Brenner, April 1977. (PB 268 740)
119 Relative Frequency of Occurrence of Warm Season Echo Activity as a Function of Stability Indices Computed from the Yucca Flat, Nevada, Rawinsonde. Darryl Randerson, June 1977. (PB 271 290/AS)
121 Climatological Prediction of Cumulonimbus Clouds in the Vicinity of the Yucca Flat Weather Station. R.F. Quiring, June 1977. (PB 271 704/AS)
122 A Method for Transforming Temperature Distribution to Normality. Morris S. Webb, Jr., June 1977. (PB 271 742/AS)
124 Statistical Guidance for Prediction of Eastern North Pacific Tropical Cyclone Motion - Part I. Charles J. Neumann and Preston W. Leftwich, August 1977. (PB 272 661)
125 Statistical Guidance on the Prediction of Eastern North Pacific Tropical Cyclone Motion - Part II. Preston W. Leftwich and Charles J. Neumann, August 1977. (PB 273 155/AS)
126 Climate of San Francisco. E. Jan Null, February 1978. Revised by George T. Pericht, April 1988. (PB88 208624/AS)
127 Development of a Probability Equation for Winter-Type Precipitation Patterns in Great Falls, Montana. Kenneth B. Mielke, February 1978. (PB 281 387/AS)
128 Hand Calculator Program to Compute Parcel Thermal Dynamics. Dan Gudgel, April 1978. (PB 283 080/AS)
129 Fire whirls. David W. Goens, May 1978. (PB 283 866/AS)
130 Flash-Flood Procedure. Ralph C. Hatch and Gerald Williams, May 1978. (PB 286 014/AS)
131 Automated Fire-Weather Forecasts. Mark A. Mollner and David E. Olsen, September 1978. (PB 289 916/AS)
132 Estimates of the Effects of Terrain Blocking on the Los Angeles WSR-74C Weather Radar. R.G. Pappas, R.Y. Lee, B.W. Finke, October 1978. (PB 289767/AS)
133 Spectral Techniques in Ocean Wave Forecasting. John A. Jannuzzi, October 1978. (PB291317/AS)
134 Solar Radiation. John A. Jannuzzi, November 1978. (PB291195/AS)
135 Application of a Spectrum Analyzer in Forecasting Ocean Swell in Southern California Coastal Waters. Lawrence P. Kierulff, January 1979. (PB292716/AS)
136 Basic Hydrologic Principles. Thomas L. Dietrich, January 1979. (PB292247/AS)
137 LFM 24-Hour Prediction of Eastern Pacific Cyclones Refined by Satellite Images. John R. Zimmerman and Charles P. Ruscha, Jr., January 1979. (PB294324/AS)
138 A Simple Analysis/Diagnosis System for Real Time Evaluation of Vertical Motion. Scott Heflick and James R. Fors, February 1979. (PB294216/AS)
139 Aids for Forecasting Minimum Temperature in the Wenatchee Frost District. Robert S. Robinson, April 1979. (PB298339/AS)
140 Influence of Cloudiness on Summertime Temperatures in the Eastern Washington Fire Weather district. James Holcomb, April 1979. (PB298674/AS)
141 Comparison of LFM and MFM Precipitation Guidance for Nevada During Doreen. Christopher Hill, April 1979. (PB298613/AS)

NOAA Technical Memorandum NWS WR-207

THE LAS VEGAS McCARRAN INTERNATIONAL AIRPORT MICROBURST OF AUGUST 8, 1989

Carven A. Scott

Weather Service Nuclear Support Office
Las Vegas, Nevada
June 1990

This publication has been reviewed and is approved for publication by Scientific Services Division, Western Region

Kenneth B. Mielke, Chief
Scientific Services Division
Salt Lake City, Utah

TABLE OF CONTENTS

LIST OF TABLES

LIST OF FIGURES

THE LAS VEGAS McCARRAN INTERNATIONAL AIRPORT MICROBURST OF AUGUST 8, 1989

I. INTRODUCTION

On August 8, 1989, the Las Vegas area experienced at least two severe microbursts. The first occurred at the Henderson Sky Harbor Airport south of the city (Figure 1), with the second at McCarran International Airport minutes afterward. Wind gusts of 46 m sec^{-1} (90 kt) were measured at McCarran International Airport by the Federal Aviation Administration (FAA) wind indicator at midfield. In addition, an abrupt wind shift near the end of the microburst event resulted in an approximate net change of over 67 m sec^{-1} (130 kt) down the active runway over a period of about five minutes.

Total damage at both airports was estimated to be 14 million dollars. Approximately 82 damaged aircraft were included in this estimate. Fortunately, there were no injuries or deaths reported with either microburst. However, two aircraft did experience extreme difficulty during takeoff and landing operations during the initial phase of the McCarran microburst.

II. DEFINITIONS

The downburst, a concentrated downdraft that can occasionally be produced by a thunderstorm, has been the object of meteorological research for several decades. The most severe form of the downburst, the microburst, has been identified as a contributing factor in a number of commercial aircraft accidents (Caracena et al. 1989). The accidents are usually the result of a loss of lift during takeoff or landing, when the aircraft enters a region of rapid change in both wind speed and direction (Figure 2). The danger to aircraft is the severe low-level wind shear associated with the microburst over small spatial scales (4 km or less).

Downbursts have been categorized according to their spatial and temporal scales (Fujita, 1985) (Table 1). In the context of the planetary scale, a macroburst is defined as a mesoscale downburst. The leading edge of the macroburst outflow at the earth's surface, labeled the gust front, is often detected by radar or is analyzed as a mesoscale feature on synoptic scale surface charts. The gust front is usually the product of downbursts from multiple thunderstorm cells.

The microburst, however, is defined as a misoscale downburst. The localized spatial and temporal nature of the microburst renders it nearly impossible to detect using present meteorological remote sensing tools; e.g., incoherent radar, satellite imagery, etc. Furthermore, microbursts quite often are products of innocuous-looking clouds (Mielke et al. 1987 and Brown et al. 1982), especially in the western United States.

III. PHYSICAL DESCRIPTION OF THE MICROBURST

Though the actual structure of the microburst may be quite complex, a general description of the microburst life cycle is depicted in Figure 3 (after Fujita, 1985). The intense, jet-like downdraft strikes the ground much like the model of steady fluid flow impacting a solid flat plate. An impact pressure field causes the downflow component to decelerate as air approaches the surface, and the horizontal component

of the wind to accelerate outward from the impact center (Caracena, 1989).

Notice in Figure 4 the vortex ring structure of the microburst surrounding the downdraft core. This feature is believed to be caused by vortex instability generated at the edges of the microburst by the return updraft (Caracena, 1982).

As the microburst strikes the surface of the earth, theory indicates that the vortex ring spins up at the periphery (Figure 5). The dynamics of this expanding ring in the deformation field at the base of a strong downdraft in the vortex ring model may explain why a microburst is observed to strengthen as it expands after surface impact (Wilson et al. 1984). Recent photographs of visible dust generated by microbursts in the Denver area have confirmed the ring structure (Fujita, 1985).

One or more vortex rings may be initiated in a microburst. The vortex ring, or rings can continue to expand, and spread outward near the ground until the downdraft ceases supplying mass. At this point the microburst usually dissipates rapidly. The sequence of events described above typically lasts about five minutes.

IV. MICROBURST ENVIRONMENT

Microbursts have been broken down into three categories (Caracena et al. 1989) according to the environments that produce them: extreme wet, extreme dry, and intermediate environment. The dry convective environment and the intermediate environment produce the vast majority of microbursts in the western United States.

The dry convective environment (Figure 6), where moist convection is typically high-based, is distinguished in plots of atmospheric soundings by the "inverted V" formed by the temperature and dew-point curves. Characteristic of this profile is a deep, dry mixed layer (with a dry-adiabatic lapse rate) topped by a moist, cloud-bearing layer. The dry layer frequently exceeds 3 km in depth in the desert southwest, such that cloud bases tend to be above the 600 mb level. The deep, dry sub-cloud layer usually evaporates most of the precipitation in the microburst before the precipitation reaches the earth's surface. The evaporative cooling is the source of most of the negative buoyancy for the downward acceleration in the sub-cloud portion of the downdraft. Thus, the dry microburst is most often identified with virga, or thin rainshafts where measurable precipitation is unlikely to occur.

Dry microbursts have been studied by Brown et al. (1982), Fujita (1986), Wakimoto (1985) and others. These authors have recognized the importance of the steep sub-cloud layer lapse rate (for evaporation), and the intensity of rainfall for the production of dry microbursts. In addition, these authors focus on the importance a weak updraft plays in the eventual formation of a dry microburst. A weak updraft produces the most favorable precipitation type--the lightly rimmed snowflake--that evaporates rapidly and completely during descent (Brown et al. 1982).

Forecasting schemes based on the model of the "extreme dry" environment have been developed by Wakimoto (1985), Wilson et al. (1984), and MacDonald (1976). All of the methods depend on the existence of a moist, convectively unstable layer in the vicinity of 500 mb, and a dry, lower layer with a dry-adiabatic lapse rate.

The "intermediate environment" is similar to the "extreme dry" except that the moist, mid-level layer is deeper, and the cloud bases are lower (Figure 7). The shallower, sub-cloud layer often produces heavy rains normally associated with the "extreme wet" microburst. It is believed

some of the processes important in the "extreme wet" regime are also present in the "intermediate environment."

Charba (1974) noted that the source of downdraft air in Oklahoma thunderstorms (intermediate, or extreme wet environment) was environmental air located between 3 km and 8 km above ground level (based on values of equivalent potential temperature). The drier, mid-level air from the near-storm environment is entrained into the cloud (Kessler, 1986), carrying the horizontal momentum of the environment. The accompanying evaporative cooling due to mixing with drier air into the thunderstorm also contributes to the negative buoyancy of the downdraft. In addition, the kinetic energy of the downdraft may be intensified by the weight of the condensation products accumulated in the warm, moist updraft. The net result of all these processes can produce wind speeds of 50 m sec^{-1}, or more at the earth's surface.

Variations of the parcel theory (Fawbush and Miller, 1954 and Foster, 1958) have been utilized as gust forecasting tools in the "wet environment" where the downdraft is assumed to remain saturated on descent to the surface. This assumption is questionable in both the dry extreme, and intermediate environment where evaporation in the sub-cloud layer enhances the downdraft.

The studies cited above indicate that meteorologists do have a reasonable understanding of the types of environments that <u>can</u> produce microbursts. However, as Caracena et al. (1989) states, "there is no simple index for estimating the potential downdraft strengths from conventional sounding and surface data."

V. CASE STUDY

A. The Synoptic Situation

Flow aloft over southern Nevada was dominated by a 500 mb anticyclone (Figures 8, 9, and 10) centered over the Arizona/Utah border at 1200 UTC on 8 August 1989.

The sounding from Desert Rock, Nevada (DRA) at 1200 UTC (Figure 11) showed a nearly saturated layer of air at about 630 mb, and another layer from 520 mb to 420 mb. Drier air existed from the surface to approximately 630 mb, and above the 420 mb level. The sounding is representative of the "intermediate environment" (Figure 7), where multiple processes may effect the strength of the microburst. This "hybrid" sounding is similar to the conditions Ellrod (1989) found in the Dallas microburst that led to a commercial airline disaster in 1985.

The Showalter and Lifted Index (Figure 12) were both zero or less, and the K Index was greater than 30 across much of the desert southwest. The layer stability analysis (Figure 13) also indicated an unstable air mass (layer stability is defined as the difference in the mean potential temperature between the 850-500 mb layer and the 700-300 mb layer. Small values imply instability while large values imply stability). These conditions were suggestive of a large area of mid-level potential instability.

At 1200 UTC satellite images and lightning detection maps (Figures 14 and 15) revealed areas of dissipating convection across south-central Nevada, and in the Sierra Nevadas. Another line of convection, apparently initiated earlier that day at about 0300 UTC (Figures 16, 17, and 18) in the vicinity of Prescott, Arizona, from the outflow boundary of a mesoscale convective system (MCS) to the south, was evident over northwestern Arizona. This line was drifting northwestward at 3 to 4 m sec^{-1} as it slowly dissipated. Surface dew points remained unusually high (13°C to 18°C) throughout the day across the desert

southwest at least partly due to the precipitation from the nocturnal thunderstorm activity.

The dissipating area of convection moved out of northwest Arizona and into the Las Vegas area by 1700 UTC (Figure 19). The dissipating line of towering cumulus and cumulonimbus arched from about Mesquite, Nevada to Las Vegas, southwestward to near Twentynine Palms, California.

Thunderstorms began forming over the high terrain of southern California by 1900 UTC, along the old instability line (Figure 20). The convection grew steadily in areal extent as it moved northeast into the California-Nevada border area at 2330 UTC (Figure 21).

Cloud-top temperatures were near -50°C (Ellrod, personal communication), indicating cloud-top heights near 12 km (40 kft). Also evident in the 2330 UTC imagery was the extent that the convective area had developed eastward, as it moved toward the northeast.

Sounding data from DRA at 0000 UTC (Figure 22) displayed very little change from the 1200 UTC measurements. Apparent, though, was a slight increase in precipitable water (from 0.97 to 1.09 inches) due to slightly higher mixing ratios through the sounding, and a deeper mid-level moisture layer. Low-level winds (below 2.5 km) had also changed from west to southwest.

The 0000 UTC (Figure 23) surface analysis exhibited few unusual features, other than the high dew points. Pressure tendencies across all of the southwest were typical of the semi-diurnal effect. Also evident was the usual surface thermal low, centered in the Las Vegas area, providing a region of low-level mass convergence.

The 0000 UTC 500 mb analyses (Figures 24 and 25) revealed a weak, short-wave trough evident in the wind field stretching from near Winnemucca, Nevada into central Nevada. Also evident was a slight eastward shift of the long-wave trough along the West Coast and the ridge across the intermountain region. This shift in the synoptic pattern allowed the winds to become more southwesterly across central California into southern Nevada. However, wind speeds at 500 mb were less than 15 m sec^{-1} across the entire southwestern United States.

Analysis of the 850 mb moisture convergence field (Figure 26) revealed strong moisture flux convergence persisting in the Four Corners area. An area of moisture flux divergence had developed from near Las Vegas, south along the Colorado River in northwest Arizona.

At 500 mb moisture flux convergence (Figure 27) was apparent in a band from the San Diego, California area across Las Vegas into southern Utah. It should be noted that the 500 mb moisture flux convergence corresponded closely with the convective activity, and short-term development on the 0030-0430 UTC satellite imagery (Figures 28 and 29).

B. The Microburst Event

Between 1931 UTC (Figure 20) and 2330 UTC (Figure 21) thunderstorm activity developed rapidly along the California/Nevada border and to the east of Desert Rock. A region of thunderstorm activity had moved as far north and east as the Spring Mountains and the McCullough Range to the west and southwest of Las Vegas (Figure 28) by 0030 UTC. WSO Las Vegas radar observed the thunderstorm activity as mainly VIP level 2 cells, occasionally reaching VIP level 3. The activity was moving northward at about 5 m sec^{-1}.

At approximately 0045 UTC, an observer in the McCarran control tower reported a thunderstorm 4 to 6 km wide, about 12 km south of the airport (Figure 1). A single, narrow rain shaft was observed to be reaching the ground at the Sky Harbor-Henderson Airport, raising a dust cloud that was moving fast enough to permit the motion to be perceived. Upon noticing the dust cloud, the controllers immediately issued a wind advisory for McCarran International Airport, switched the active runway, and began rerouting air traffic. At this time, a strong microburst struck the Sky Harbor Airport (Figure 1), destroying numerous aircraft in the process. Within a couple of minutes, the rain shaft and dust cloud were observed by the controllers to dissipate. Consequently, the controllers reopened runway 19 and cancelled the wind advisory for McCarran International Airport.

The thunderstorm continued to approach McCarran International Airport from the south. The National Weather Service observer reported thunder, with a light rain shower, beginning at 0049 UTC. Southeast winds had increased and were 10 m sec^{-1} gusting to 22 m sec^{-1} (Appendix A).

Cloud-to-ground (CG) lightning had also begun to increase in the thunderstorm cluster from one CG flash every four to five minutes to about one per minute by 0050 UTC. In the ensuing eight minutes, CG flash frequency increased to three per minute and peaked at six flashes per minute within the cluster at 0101 UTC (Appendix B).

At approximately 0100 UTC, the control tower observer reported the rapid formation and northward movement of a dust cloud just to the south of the active runway 19. A commercial airliner was in the process of taking off and reported extreme turbulence flying through the cloud. It was at this time the Low-Level Windshear Alert System (LLWAS) sensor at the end of runway 19 activated an alarm in the control tower (Figure 30).

The dust cloud moved rapidly toward the control tower arriving at approximately 0103 UTC. Heavy rain and zero visibility were reported from the tower within seconds of the arrival of the wind and dust. FAA wind equipment, located at mid-field, registered a wind gust to 46 m sec^{-1} from the south-southeast. Tower personnel reported pronounced swaying of the tower due to the strong wind. Reliable eyewitnesses near the airport observed the "boiling" sand cloud near the ground as it moved through the airport.

NWS wind equipment, collocated with FAA mid-field equipment, registered a gust to 40 m sec^{-1} before losing power at approximately 0105 UTC. A lightning bolt struck near the back-up power generator, knocking out all power and telephones to the WSO at the Hughes Air Terminal on the west side of the airport (Figure 30).

At the height of the event, tower personnel observed the wind direction from the LLWAS equipment around the airport. The wind pattern at that time (Figure 31) indicated the characteristic footprint of a microburst.

At approximately 0107 UTC, wind gusts decreased to about 26 m sec^{-1}, and abruptly switched to the north. After another two to three minutes, winds diminished to about 2 m sec^{-1}, and switched to southerly again. The entire episode lasted no more than 10 minutes. Rainfall during the brief event was quite heavy for the desert, totaling .41 inches.

The temperature dropped dramatically between 0050 UTC and 0106 UTC from 31.5°C to 19.5°C. The maximum temperature at the airport was 38.0°C prior to the arrival of the thunderstorm activity. Utilizing the Fawbush and Miller

(1967) graphical technique for "wet" microbursts, results in a forecast peak gust of 39.6 m sec^{-1} ±3 m sec^{-1}. Utilizing Randerson's technique (1982) developed for estimating gusts in desert thunderstorms yields a peak gust of 25 m sec^{-1} ±6 m sec^{-1}.

A barograph trace (Figure 32) was also available during the episode and showed a very strong pressure jump of about 0.20 inches (6.7 mb) associated with the microburst. Employing Bernoulli's equation, a maximum wind estimate of 33.1 m sec^{-1} is obtained due to the negative buoyancy in the downdraft (for an explanation of Bernoulli's equation, see Appendix C). Unfortunately, due to the coarse time resolution on the graph, it is impossible to know exactly when the peak pressure occurred.

C. Damage Report

Reports from the Sky Harbor Airport revealed that numerous aircraft were damaged in the microburst. However, ground reports between the two airports show no evidence of damage or severe winds (Figure 1).

The second microburst was also fairly limited in areal extent, extending from near the south end of runway 19 along Sunset Road to just northeast of the airport on Maryland Parkway (Figure 30). A commercial pilot who lives just to the southwest of the airport (Figure 33) observed the entire episode and reported only a sprinkle of rain with winds under 5 m sec^{-1}. This report is similar to the one from an airport employee who witnessed the event from approximately 7 km south of the McCarran International Airport (Figure 33).

The microburst did considerable damage to several aircraft hangars on the west side of the McCarran International Airport. Numerous small aircraft were either damaged or destroyed by the winds. The microburst apparently dissipated just to the northeast of the airport. However, this was not before knocking down 12 power poles (Figure 30) along Maryland Parkway. Power service was disrupted at the airport, a few businesses, and numerous residential customers due to the downed power lines.

Approximately 14 million dollars in damages resulted from these two microbursts. This estimate includes severe damage to several hangars, 80 aircraft (that were reportedly tied down), and power lines. Fortunately, there were no reported deaths or injuries.

VI. SUMMARY

Atmospheric stability and moisture content over southern Nevada on this day (Figures 11 and 22) were very similar to that observed near Dallas-Fort Worth (Figure 7) on the day a severe microburst occurred there. However, at the present time, there is no simple index to accurately forecast the maximum wind gust in a microburst from a sounding. The indices require a forecast of the storm environment, e.g., surface potential temperature, in order to be of much use. Alert, accurate, and timely observations remain the most vital tool in forecasting and nowcasting of microburst events.

Suggestive of microburst potential may have been the strong moisture flux divergence at 850 mb across southern Nevada. This was coupled with the moisture flux convergence band at 500 mb across southern Nevada. Further study will be required to determine the viability of these as indicators of microburst potential.

Unfortunately, there is no evidence to establish that the thunderstorm which produced the microbursts in Las Vegas manifested any meteorologically significant radar signatures; e.g., an intense

reflectivity return, a hail spike, or an extraordinary radar top. The WSO Las Vegas WSR-74C is a local radar, and therefore, was not manned at the time of the event. The network radar watch (WSO Palmdale) responsible for the Las Vegas area (Figure 34) is not suited for monitoring short-fused, small-scale meteorological events such as a microburst. The sensitivity-time control (STC) curves, and the wide vertical beam width (6 to 7 degrees) of FAA radars are inadequate for short-range observations. In any event, neither radar archives data with sufficient frequency to be of use in the post-storm reconstruction of this event.

As stated previously, investigators have pointed out microbursts spawned by the "dry extreme" and the "intermediate" environment are often the products of parent clouds that are not severe. The thunderstorm that produced the microburst resulting in a commercial airliner disaster at the Dallas-Fort Worth Airport was observed as a small shower (approximately 30 dBZ) with a radar top of only 7 km (Fujita, 1986), minutes before the event. Rapid intensification to approximately 45 dBZ (a VIP level 4) occurred only four minutes before the microburst (Caracena et al. 1986).

Recent work by Williams and Orville (1988) and Beuchler et al. (1988), point to a relationship between intracloud (IC) lightning and microbursts in the "extreme wet" environment. IC activity maximizes four to 10 minutes prior to the time of maximum outflow at the surface due to charge separation processes occurring in the thunderstorm updraft. It is unknown if this technique would be useful in either the "dry extreme" or the "intermediate" environments. A potentially, inexpensive procedure to test this principle would be to combine output from an optical detector (Scott, 1989) with real-time CG lightning flash data. A simple algorithm could be programmed into a personal computer that would subtract the CG lightning data set from the full lightning spectrum collected by the optical device. The product would be an estimate of the real-time IC lightning frequency in the vicinity of the optical detector.

There is sufficient knowledge of the microburst in dry and intermediate environments to issue an "area-wide microburst alert" based on vertical moisture and temperature profiles (Wilson et al. 1984 and Caracena et al. 1989). The microburst alerts would heighten the level of awareness in the aviation community, both FAA and pilots.

Numerous authors have cited the tendency for microbursts to occur in families. Wilson et al. (1984) found in a study of the Denver Airport area that in 71 microbursts examined, 70 percent occurred on days when three or more were observed on the same day. The lesson is that when one microburst is observed, vigilance levels for other occurrences should be increased. Thus, upon the occurrence of a microburst event, an "area-wide microburst alert" could be upgraded to an "area-specific warning".

VII. RECOMMENDATIONS

- As Smith (1986) asserted, classify microbursts as an observable phenomena. Visual identification of microbursts may be the final line of defense in avoiding a microburst-related accident or disaster.

- Further investigation of a cost-effective, "total lightning rate" detector is vital. Unknown is the effectiveness of the IC lightning rate observation in the western states as a microburst precursor.

- More emphasis should be placed on microburst identification and forecasting techniques in both FAA and NWS training courses.

VIII. APPENDICES

```
SA 0050 E150 BKN 250 BKN 15 066/93/49/3409/983/ 107 1072 (HCB)
SA 0150 E150 BKN 250 BKN 15 076/93/49/1408/986/CB DSNT SE OCNL LTGCCIC (HCB)
SP 0230 E120 BKN 150 BKN 15T 1416/988/TB25 CB OVHD MOVG NW FQT LTGCCIGCG (HCB)
SA 0250 E100 OVC 6TRW 096/79/63/2226637/991/RB25 CB OVHD MOVG NW FQT LTGICCCCG OCNL RW+ (HCB)
SA COR 0250 E100 OVC 6TRW 096/79/63/2226637/991/RB25 CB OVHD MOVG NW FQT LTGCCICCG OCNL RW+ PK WND 2237/46 (HCB)
RS 0352 E100 BKN 150 BKN 250 BKN 15 095/80/61/2410/991/TE45 MOVG N OCNL LTGICIC RE45/ 12435 1963 78 20035 (JWS)

72386 11974 62410 10267 20161 39353 40095 51024 60091 72992 85963 333 10428 20256 70089 90551 555 90812= (JWS)

RS COR 0352 E100 BKN 150 BKN 250 BKN 15 095/80/61/2410/991/TE45 MOVG N OCNL LTGICCG RE45/ 12435 1963 78 20035 (JWS)

72386 11974 62410 10267 20161 39353 40095 51024 60091 72992 85963 333 10428 20256 70089 90551 555 90812= (COR) (JWS)

SA 0450 E100 BKN 150 BKN 250 BKN 50 102/80/62/2710/992/CB W-N-E MOVG N FQT LTGCCCG (JWS)
SA 0550 100 SCT E150 BKN 250 BKN 50 109/80/64/3209/994/CB N DSIPTG RWU NW-E (JWS)
SA 0650 120 SCT E150 BKN 250 BKN 25 115/81/65/1409/996/ 217 1273 (HCB)
SA 0750 E150 BKN 250 BKN 35 114/86/63/3605/996/RWU NE-SE (JWS)
SA 0850 E130 BKN 250 OVC 35 115/86/64/0305/996/MDT CU OMTNS W-NE RWU DSNT E (FDT)
SA 0950 E130 BKN 250 OVC 35 110/88/66/0909/995/TCU S-N BINOVC/ 803 1271 78 (JWS)

72386 32985 00909 10311 20189 39367 40110 58003 81271 333 10350 20256 70089 555 90810= (JWS)

SA 1050 E130 BKN 250 OVC 35 106/91/63/0509/994/TCU S AND NW BINOVC (JWS)
SA 1150 130 SCT E250 OVC 35 097/93/60/0909/991/MDT CU N BINOVC (JWS)
SA 1250 90 SCT 130 SCT E250 BKN 35 084/99/61/0905/988/TCU S-N/ 722 1268 (JWS)
SA 1350 90 SCT 130 SCT E250 BKN 35 075/98/61/0907/985/CB DSNT NE TCU ALQDS (FDT)
SA 1450 90 SCT E250 BKN 35 065/100/59/2106/982/CB OMTNS W-NE RWU DSNT W (FDT)
SA 1552 100 SCT 140 SCT E250 OVC 35 060/99/56/1811/980/CB NW AND NE/ 725 1350 00 (LED)

72386 32985 01811 10372 20133 39319 40060 57025 82350 333 10370 20256 70089 555 90900= (LED)

SA 1650 E100 BKN 140 OVC 35TRW- 067/89/61/1420642/981/TB49 SE MOVG N RB49 (LED)
SA COR 1650 E100 BKN 140 OVC 35TRW- 067/89/61/1420642/981/ TB49 SE MOVG N RB49 PEAK WND 1442/33 (LED)
RS COR 1650 E100 BKN 140 OVC 35TRW- 067/89/61/1420642/981/TB49 SE MOVG N RB49 PEAK WND 1442/33 (CHS)
SP 1705 W0 X 0T+RW+ 1435678/981/T ALQDS CONT LTGCG ALQDS (CHS)
SP 1715 E90 OVC 35TRW- 0000/981/CB ALQDS T N MOVG N OCNL LTGCG N (CHS)
SP 1734 E90 BKN 150 BKN 250 OVC 35 0000/981/CB ALQDS TE30 MOVD N RE30 OCNL LTGCG N (CHS)
SA 1750 90 SCT E150 BKN 250 OVC 35 072/76/70/0000/981/CB ALQDS MOVG N RWU N OCNL LTGCG N TRE30 PK WND 1478/03 (CHS)
SA 1853 90 SCT 150 SCT E250 OVC 35 080/84/69/0000/984/CB RWU N MOVG N/ 31441 1963 (CHS)
SA 1955 150 SCT E250 BKN 15 085/83/66/2405/986/CB OCNL LTGIC DSNT W (CHS)
SA 2055 150 SCT 250 SCT 15 076/83/64/2305/983/CB OCNL LTCCCG DSNT NE (CHS)
SA COR 2055 150 SCT 250 SCT 15 076/83/64/2305/983/CB OCNL LTGCCCG DSNT NE (CHS)
SA 2151 CLR 15 096/83/66/1903/989/CB OCNL LTGIC DSNT W/ 21741 1301 00 (CHS)

72386 11974 11903 10283 20189 39350 40096 52017 60101 70101 81301 333 10370 20194 70193 90550 555 90906= (CHS)

SA 2254 150 SCT E250 BKN 15 093/82/65/0504/989/CB OCNL LTGCCIC DSNT W (CHS)
SA 2350 90 SCT E150 OVC 15 096/82/64/0311621/990/CB OCNL LTGCCIC DSNT W/ 98513 (CHS)
```

Appendix A - Summary of Las Vegas McCarran Airport Observations on August 8, 1989

DATE	TIME	LAT	LON	DIST	DIST	AS	SIGMA	RESPD	DFS	
AUG 09 89	00:05:15	36.42	115.44	5.3	29.	2	-17.6	22	5	15
AUG 09 89	00:06:22	36.30	115.56	6.4	29.	1	-20.6	5	4	
AUG 09 89	00:07:27	36.05	115.40	7.3	18.	1	-17.6	5	34	
AUG 09 89	00:08:40	36.32	115.47	8.7	26.	1	-30.8	22	5	4
AUG 09 89	00:10:18	36.31	114.85	10.3	19.	1	-22.0	15	33	
AUG 09 89	00:13:07	36.16	115.41	13.1	29.	1	-15.0	28	5	15
AUG 09 89	00:13:40	36.40	115.47	13.7	29.	3	-26.6	22	28	5
AUG 09 89	00:16:06	35.94	115.60	16.1	30.	1	-16.8	5	22	
AUG 09 89	00:21:41	36.05	115.58	21.7	27.	1	-14.0	22	4	
AUG 09 89	00:22:29	36.25	115.24	22.6	13.	1	-44.2	22	33	6
AUG 09 89	00:28:42	36.45	115.30	28.7	26.	1	-17.0	22	34	
AUG 09 89	00:26:22	36.09	115.67	36.4	26.	7	-17.2	22	5	
AUG 09 89	00:38:06	36.04	115.62	38.1	29.	4	-23.6	5	22	
AUG 09 89	00:43:54	36.12	115.24	43.9	9.	3	-43.4	22	5	4
AUG 09 89	00:44:02	36.38	115.44	44.0	17.	1	-21.0	22	34	
AUG 09 89	00:45:29	36.08	115.57	45.5	26.	1	-15.0	22	15	
AUG 09 89	00:48:48	36.13	115.25	48.8	9.	3	-17.0	22	19	5 1
AUG 09 89	00:49:45	36.10	115.58	49.8	27.	5	-19.6	22	34	
AUG 09 89	00:50:07	36.09	115.21	50.1	7.	3	-28.2	22	19	4
AUG 09 89	00:52:47	36.00	115.04	52.8	7.	1	-16.0	22	15	
AUG 09 89	00:53:38	36.42	115.11	53.6	21.	2	-22.6	22	19	4
AUG 09 89	00:53:59	36.09	115.63	54.0	30.	6	-17.8	5	4	15
AUG 09 89	00:55:14	36.04	115.04	55.2	5.	2	-20.8	15	34	
AUG 09 89	00:55:26	36.10	115.59	55.4	27.	9	-24.0	22	15	34
AUG 09 89	00:56:53	36.35	115.35	56.9	22.	1	-13.8	22	5	
AUG 09 89	00:57:31	36.05	115.49	57.5	22.	3	-24.0	22	3	34
AUG 09 89	00:57:43	36.14	115.16	57.8	5.	1	-20.6	22	5	
AUG 09 89	00:58:46	36.01	115.02	58.8	7.	1	-14.8	15	34	
AUG 09 89	00:58:53	36.22	115.22	58.9	11.	2	-15.0	22	19	5 1
AUG 09 89	00:59:20	36.07	115.05	59.3	3.	2	-20.2	22	15	
AUG 09 89	00:59:21	35.00	115.34	59.3	15.	4	-56.4	5	19	4 1
AUG 09 89	00:59:54	36.08	115.09	59.9	1.	3	-17.6	22	5	
AUG 09 89	01:00:26	36.07	115.14	60.4	4.	2	-18.4	22	5	15
AUG 09 89	01:01:04	36.12	115.17	61.1	5.	2	-13.0	22	5	15
AUG 09 89	01:01:34	36.10	115.01	61.6	4.	2	-22.0	28	5	15
AUG 09 89	01:01:34	36.14	115.40	61.6	17.	1	-26.2	15	28	
AUG 09 89	01:01:54	36.38	115.42	61.9	26.	3	-18.8	22	5	4 1
AUG 09 89	01:01:55	36.09	115.06	61.9	1.	4	-14.6	22	5	
AUG 09 89	01:01:56	35.96	115.08	61.9	9.	1	-16.6	15	34	
AUG 09 89	01:02:42	36.10	115.09	62.7	1.	6	-21.4	22	5	15
AUG 09 89	01:02:43	36.10	115.46	62.7	20.	2	-21.0	19	28	4
AUG 09 89	01:03:06	35.96	115.06	63.1	9.	4	-41.4	22	15	15
AUG 09 89	01:04:25	36.02	115.45	64.4	21.	4	-23.0	22	14	4
AUG 09 89	01:04:46	36.18	115.18	64.8	8.	3	-97.2	22	5	19
AUG 09 89	01:04:47	36.21	115.43	64.8	20.	1	-42.2	33	19	
AUG 09 89	01:05:06	36.13	115.18	65.1	6.	2	-87.0	22	5	4 1
AUG 09 89	01:06:42	36.19	115.23	66.7	10.	1	-16.8	22	5	15
AUG 09 89	01:07:43	35.99	115.29	67.7	13.	2	-22.2	5	28	4 1
AUG 09 89	01:08:26	36.03	115.27	68.4	11.	6	-16.0	5	28	15
AUG 09 89	01:08:54	36.11	115.00	68.9	4.	3	-17.6	22	15	34
AUG 09 89	01:08:54	36.07	115.33	68.9	14.	1	-13.6	5	28	4
AUG 09 89	01:09:33	36.19	115.13	69.5	7.	3	-19.8	22	15	
AUG 09 89	01:10:23	36.14	115.06	70.5	3.	3	-18.4	22	5	15
AUG 09 89	01:10:23	36.02	115.35	70.5	15.	1	-23.6	28	4	
AUG 09 89	01:11:07	36.18	115.26	71.1	11.	4	-20.0	22	19	5 1
AUG 09 89	01:11:42	35.84	115.21	71.7	19.	4	-28.0	28	15	34
AUG 09 89	01:11:43	36.15	115.10	71.7	3.	3	-39.0	5	24	4
AUG 09 89	01:12:54	35.94	115.30	72.9	16.	1	-21.8	5	28	15
AUG 09 89	01:13:03	36.12	114.97	73.0	6.	3	-20.0	5	15	
AUG 09 89	01:13:40	36.11	115.31	73.7	12.	2	-32.0	19	28	4
AUG 09 89	01:14:53	36.11	115.25	74.9	9.	2	-26.0	5	19	4 1
AUG 09 89	01:15:14	36.06	115.29	75.2	12.	2	-43.4	5	28	4 1
AUG 09 89	01:16:24	36.17	115.37	76.4	16.	2	-47.2	30	19	5 1
AUG 09 89	01:17:02	35.96	115.25	77.0	13.	1	-17.8	5	28	15
AUG 09 89	01:18:22	36.19	115.29	78.4	13.	3	-24.0	5	34	35
AUG 09 89	01:18:22	36.49	115.07	78.4	26.	2	-20.0	19	15	
AUG 09 89	01:18:23	36.04	115.30	78.4	12.	1	-23.0	28	4	33
AUG 09 89	01:19:10	36.19	115.16	79.2	7.	2	-27.4	22	5	4 1
AUG 09 89	01:19:10	36.31	115.47	79.2	25.	1	-21.2	19	28	
AUG 09 89	01:19:26	36.17	115.20	79.4	8.	1	-19.8	22	5	15
AUG 09 89	01:20:37	36.21	115.14	80.6	8.	2	-17.8	22	5	
AUG 09 89	01:20:54	36.42	115.26	80.9	23.	1	-24.0	22	5	19
AUG 09 89	01:21:55	36.24	115.23	81.9	12.	6	-34.4	22	5	3
AUG 09 89	01:22:18	36.29	115.20	82.3	14.	4	-20.4	22	5	15
AUG 09 89	01:22:33	36.14	115.09	82.5	3.	2	-17.2	22	15	
AUG 09 89	01:23:05	36.23	115.13	83.1	10.	1	-18.8	22	5	
AUG 09 89	01:26:08	36.54	115.11	86.1	29.	1	-22.2	19	5	15
AUG 09 89	01:27:14	36.38	115.33	87.2	23.	2	-19.8	22	19	5 1
AUG 09 89	01:27:55	36.41	115.20	87.9	22.	1	-20.0	22	19	4
AUG 09 89	01:28:27	36.45	115.18	88.5	24.	2	-18.8	22	19	5 1
AUG 09 89	01:29:14	36.27	115.15	89.2	28.	5	-41.0	22	5	19
AUG 09 89	01:29:14	36.15	115.54	89.2	25.	2	-24.6	19	4	6
AUG 09 89	01:29:24	36.37	115.18	89.4	19.	1	-16.0	22	15	
AUG 09 89	01:29:33	36.21	115.43	89.5	20.	2	-21.0	5	4	35
AUG 09 89	01:29:41	36.47	115.17	89.7	25.	2	-24.6	22	19	5 1

Appendix B - Summary of Cloud-to-Ground Lightning Flashes from 0000 UTC - 0130 UTC on August 9, 1989

APPENDIX C.

The generalized form of the equation for steady, nonviscous, incompressible fluid flow (Lamb, 1945) can be written as:

(1) $$\int Dp/P + \Omega + \tfrac{1}{2}v^2 = \text{constant}$$

where,

p = pressure
P = density
Ω = velocity potential
v = velocity.

This equation, called *Bernoulli's equation*, shows that the pressure varies inversely to the velocity of the fluid along any one streamline.

Bernoulli's equation can be simplified for application in a microburst (Fujita, 1985) as:

(2) $$p = \tfrac{1}{2}Pv^2$$

where,

p = static pressure change
P = density
v = velocity.

This equation (Figure 34) expresses the **measured** pressure change at any point as a simple function of the wind speed.

The total pressure, a sum of the static and velocity pressure, remains constant during a frictionless outflow from the microburst (Figure 34). Barometers measure static pressure, which varies as a function of wind velocity.

For the event at McCarran International Airport on August 8, 1989, the measured static pressure change at the barograph was approximately 6.7 mb. Using equation (2), with a range of densities appropriate for the ambient temperature and elevation, the maximum wind speed expected would be about 33 m sec^{-1}.

IX. ACKNOWLEDGEMENTS

My sincere thanks to J. M. Fair, Dr. D. Randerson, and J. Rea of WSNSO for their helpful comments while reviewing the paper. Additional thanks to R. Holle and F. Caracena of NOAA/ERL, R. Thompson WSFO/Reno, and G. Ellrod of NOAA/NESDIS, and W. Rogers of NWS/CWSU for their suggestions. A special thanks to S. Keighton and C. Hill of WR/SSD, F. Taylor of WSO/Las Vegas, T. Ross of NCDC, and R. Earl and D. Norton of the FAA for their invaluable assistance constructing the data sets and reconstructing the events on August 8, 1989.

X. REFERENCES

Brown, J. M., K. R. Knupp, and F. Caracena, 1982: Destructive Winds From Shallow, High-based Cumulonimbi, Preprints, 12th Conference on Severe Local Storms, 272-275.

Beuchler D. E., S. J. Goodman, and M. E. Weber, 1988: Cloud-to-Ground Lightning Activity in Microburst-producing Storms, Preprints of the 15th Conference on Local Storms, 196-201.

Caracena, F., R. Holle, C. Doswell, 1989: Microbursts - A Handbook For Visual Identification. NOAA/ERL/NSSL Handbook, 35.

Caracena, F., 1982: Is the Microburst a Large Vortex Ring Imbedded in a Thunderstorm Downdraft? (abstract only). *EOS-Transactions of the American Geophysical Union,* **63**, 89.

Caracena, F., R. Ortiz, and J. A. Augustine, 1986: The Crash of Delta Flight 191 at Dallas-Fort Worth International Airport on 2 August 1985: Multi-scale Analysis of Weather Conditions, NOAA Technical Report ERL 430-ESG 2, Environmental Sciences Group, Boulder, CO, 33.

Charba, J., 1974: Application of Gravity Current Model to Analysis of Squall-line Gust Front, *Monthly Weather Review,* 86, 91-94.

Ellrod, G., 1989: Dallas Microburst Storm Environmental Conditions Determined From Satellite Soundings, Preprints of the Third International Conference on the Aviation Weather System, 15-20.

Ellrod, G., 1989: Personal Communication.

Fawbush, E. J. and R. C. Miller, 1954: A Method for Forecasting Peak Gusts in Non-frontal Thunderstorms, *Bulletin of the American Meteorological Society,* 35, 14-19.

Foster, D. S., 1958: Thunderstorm Gusts Compared with Computed Downdraft Speeds, *Monthly Weather Review,* 86, 91-94.

Fujita, T., 1985: The Downburst, Microburst, and Macroburst, SMRP Research Paper No. 210 [NTIS No. PB85-148880], University of Chicago, 122.

Fujita, T., 1986: DFW Microburst on August 2, 1985. SMRP Research Paper No. 217 [NTIS No. PB86-131638], University of Chicago, 155.

MacDonald, A., 1976: Gusty Surface Winds and High Level Thunderstorms, Western Region Technical Attachment No. 76-14, U.S. Department of Commerce, National Weather Service Western Region.

Mielke, K. B., and E. Carle, 1987: An Early Morning Dry Microburst in the Great Basin, *Weather and Forecasting,* 2, 169-174.

Randerson, R., 1982: Approximations to the Peak Surface Wind Gusts From Desert Thunderstorms, NOAA Technical Memorandum NWS WR-176, U.S.

Department of Commerce, National Weather Service Western Region.

Sasaki, Y. and T. L. Baxter, 1986: The Gust Front, Thunderstorm Morphology and Dynamics, E. Kessler, ed, University of Oklahoma, p 187-196.

Scott, C. A., 1989: LIVES-88 -Verification of Detection Efficiency and Accuracy of the Nevada Test Site Automatic Lightning Detection System, Western Region Technical Attachment, No 89-20, July 25, 1989.

Smith, M., 1986: Visual Observations of Kansas Downbursts and Their Relation to Aviation Weather Observations, *Monthly Weather Review,* **114**, 1612-1616.

Smythe, G. R., 1989: Evaluation of the 12-Station Enhanced Low-Level Wind Shear Alert System (LLWAS) at Denver Stapleton International Airport, Preprints of the Third International Conference on the Aviation Weather System, 41-46.

Wakimoto, R. M., 1985: Forecasting Dry Microburst Activity Over the High Plains, *Monthly Weather Review,* **113**, 1131-1143.

Williams, E. and R. Orville, 1988: Intracloud Lightning as a Precursor to Thunderstorm Microbursts, Proceedings of the 1988 International Aerospace and Ground Conference on Lightning and Static Electricity, NOAA Special Report, 454-459.

Wilson, J. W., R. D. Roberts, C. Kessinger, and J. McCarthy, 1984: Microburst Wind Structure and Evaluation of Doppler Radar for Airport Wind Shear Detection, *Journal of Climate and Applied Meteorology,* **23**, 898-915.

Table 1

Temporal and Spatial Scales of the Microburst and the Gust Front/Macroburst

Type	Dimension	Spatial Scale	Temporal Scale
Microburst	4 km or less	Misoscale	10 minutes or less
Macroburst/ Gust Front	Greater than 4 km	Mesoscale	5 minutes to 2 hours

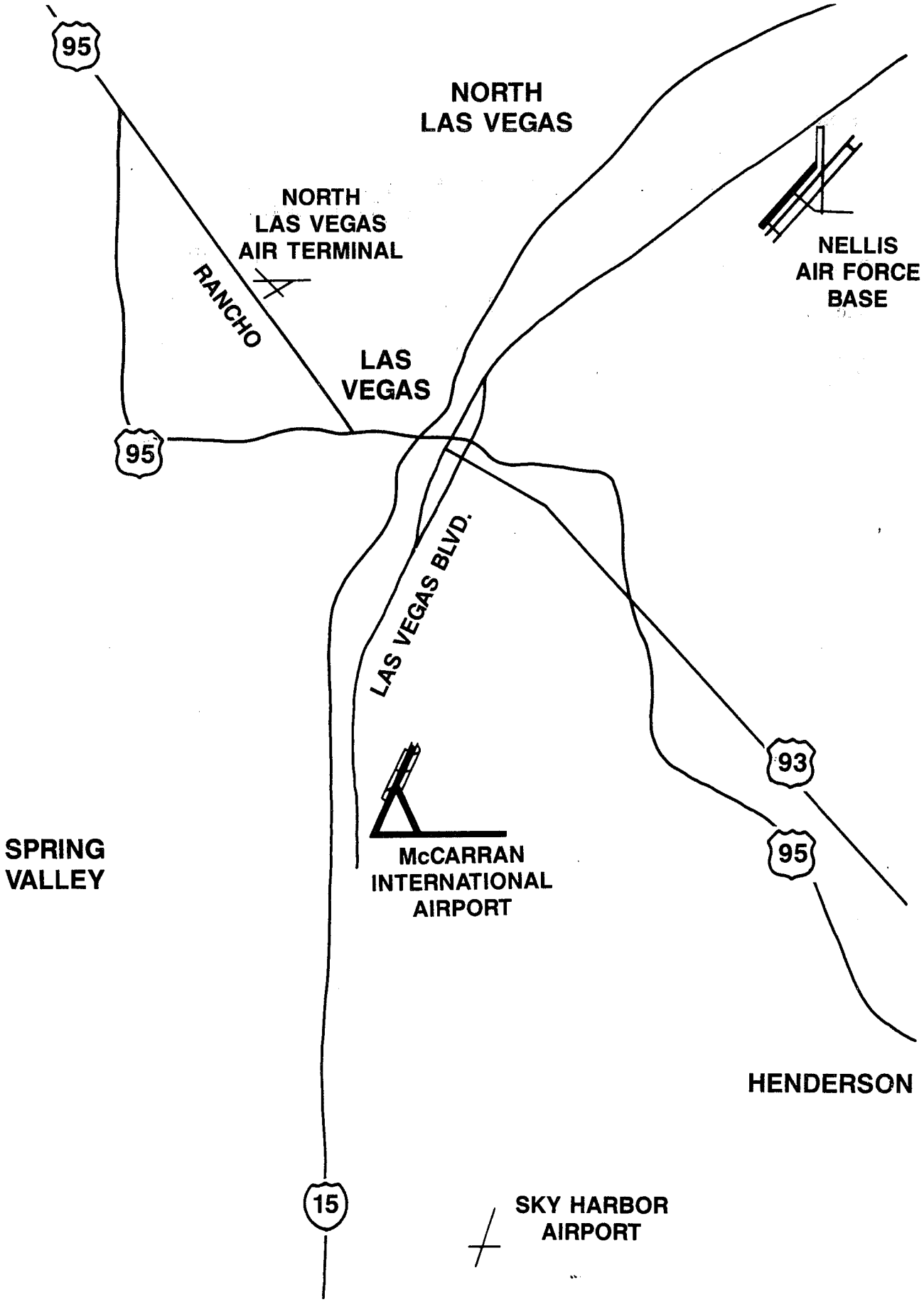

FIGURE 1
THE LAS VEGAS AREA

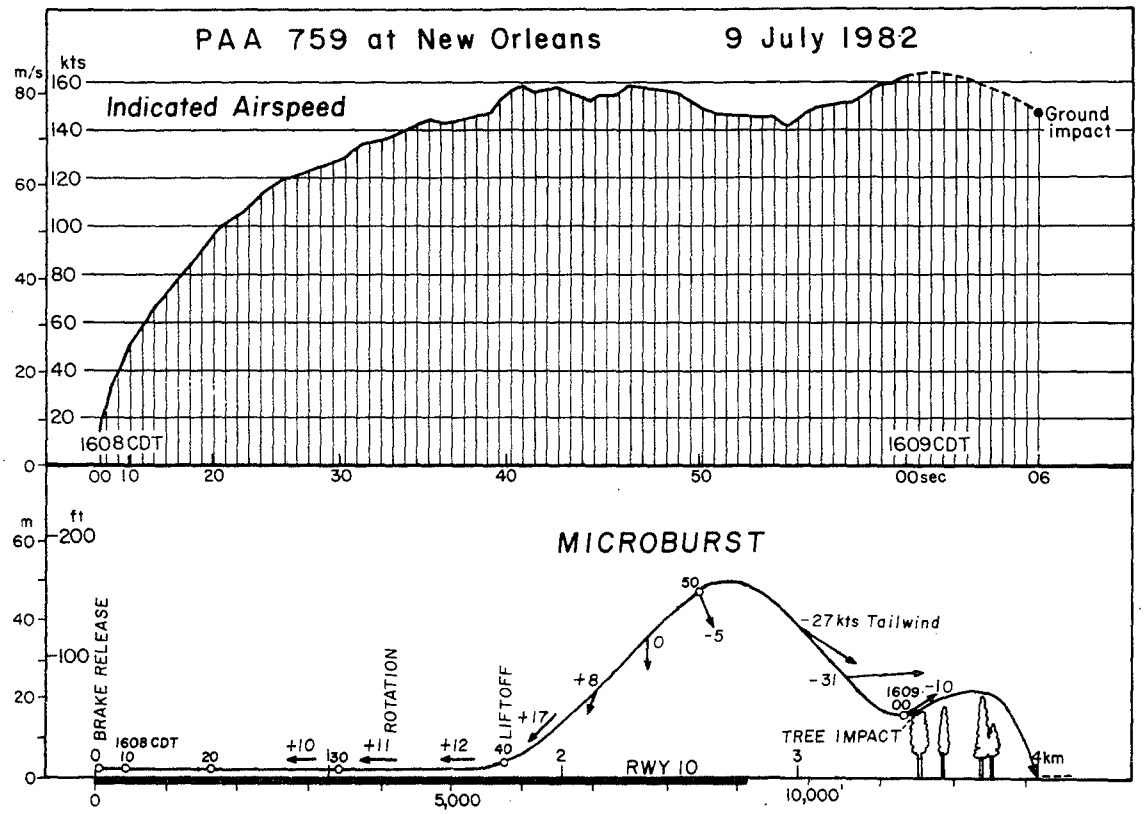

FIGURE 2
FLIGHT PATH AND INDICATED AIRSPEED OF PAA 759 AT THE NEW ORLEANS AIRPORT ON 9 JULY 1982. ACCORDING TO THE AUTHOR'S RECONSTRUCTION, THE AIRCRAFT REACHED 163 FT. (50 m) AGL. THEREAFTER, IT DESCENDED TO 52 FT. (16 m), CONTACTING A TREE ON THE EAST SIDE OF WILLIAMS BLVD. (FUJITA, 1985)

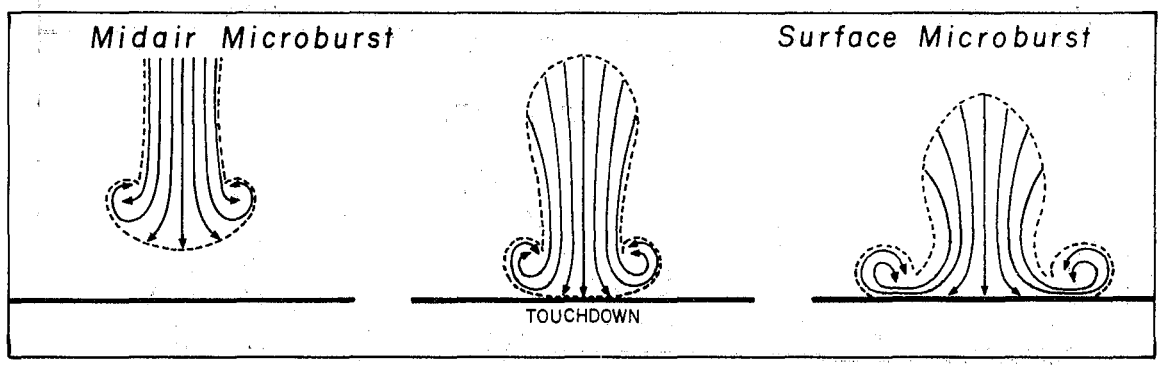

FIGURE 3
THREE STAGES OF A DESCENDING MICROBURST. A MID-AIR MICROBURST MAY OR MAY NOT DESCEND TO THE SURFACE. IF IT DOES, THE OUTBURST WINDS DEVELOP IMMEDIATELY AFTER ITS TOUCHDOWN. (FUJITA, 1985)

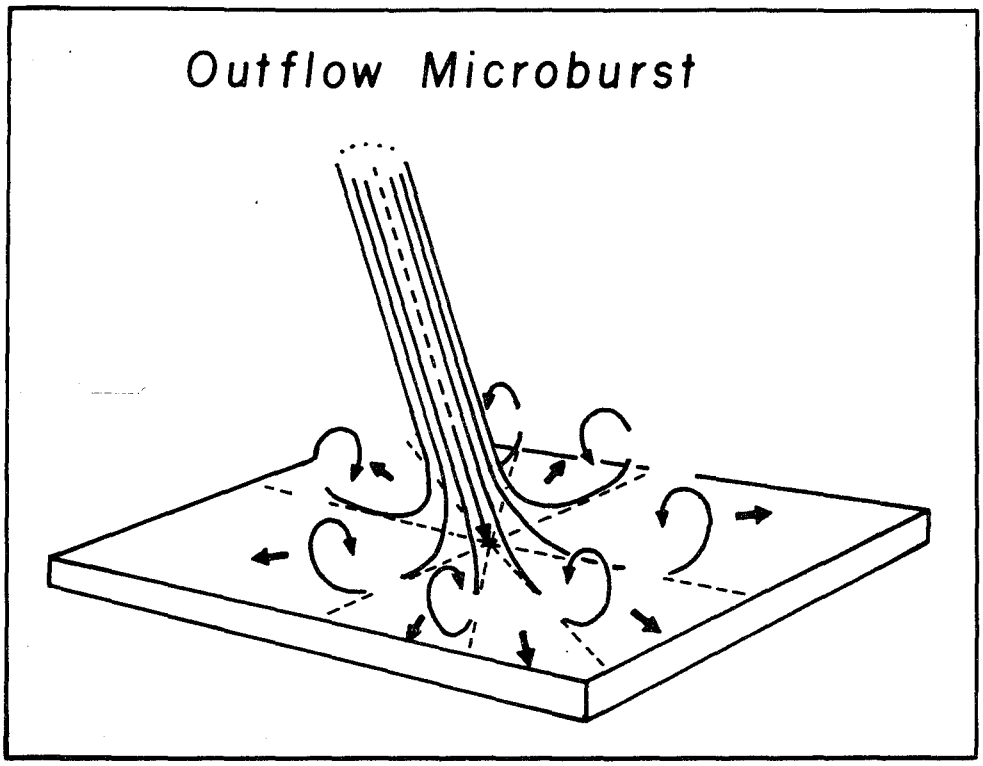

FIGURE 4
OUTFLOW MICROBURSTS ARE THE MOST COMMONLY OBSERVED TYPE OF MICROBURSTS (FUJITA, 1985)

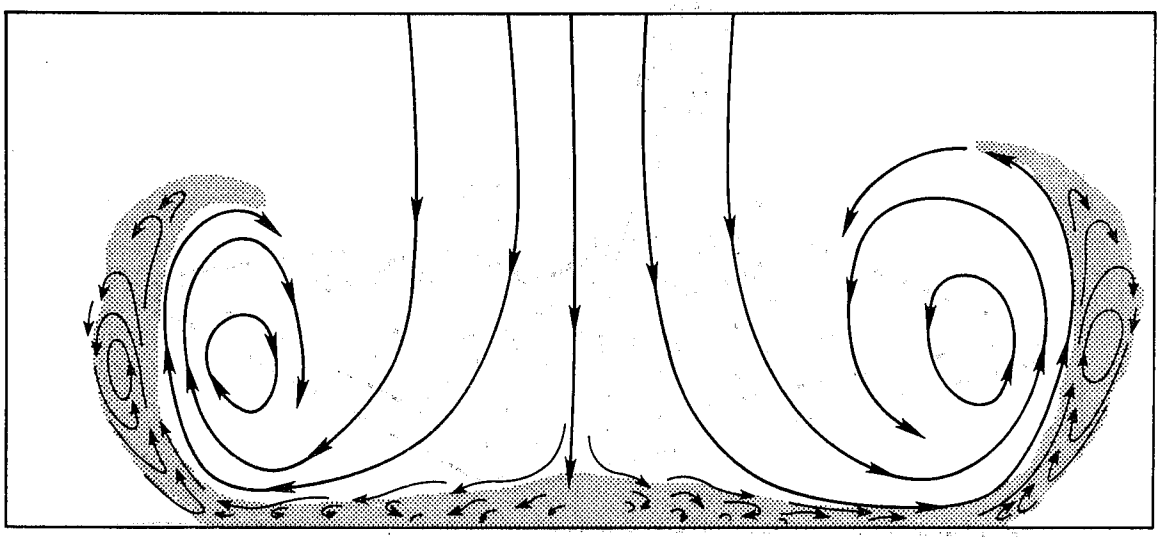

FIGURE 5
CROSS SECTION OF A CONCEPTUAL VORTEX RING MODEL OF A MICROBURST (CARACENA, 1982; 1987). THE SHADED PORTION IS THE FRICTION BOUNDARY LAYER THAT CONTAINS VORTICITY OPPOSITE TO THAT OF THE DESCENDING RING.

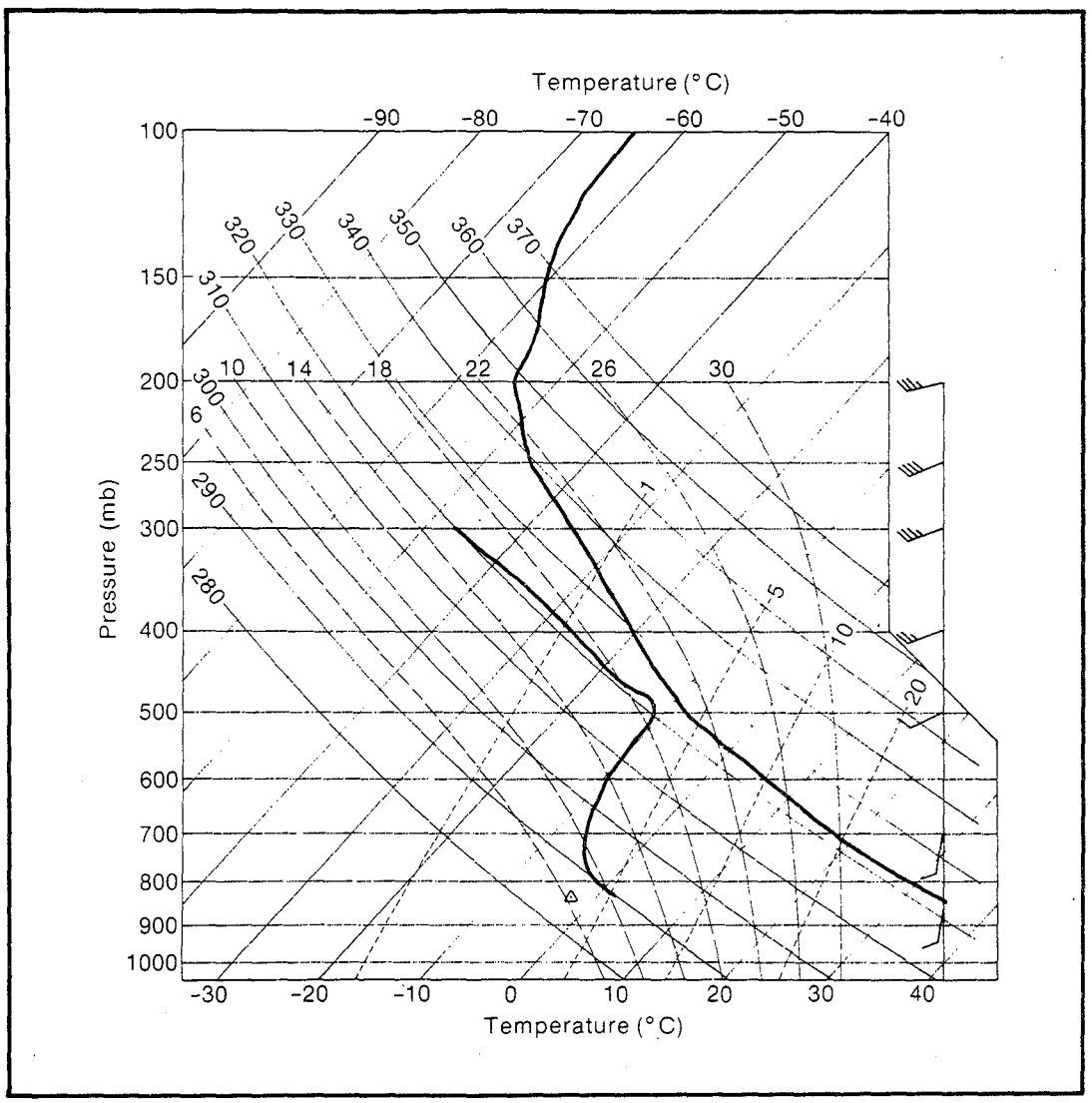

FIGURE 6
A COMPOSITE OF FIVE AFTERNOON (0000 UTC) SOUNDINGS BY BROWN et al. (1982) FOR CONVECTIVE EVENTS THAT PRODUCED DAMAGING SURFACE WINDS ASSOCIATED WITH HIGH-BASED CUMULONIMBI IN THE FRONT RANGE AREA OF COLORADO

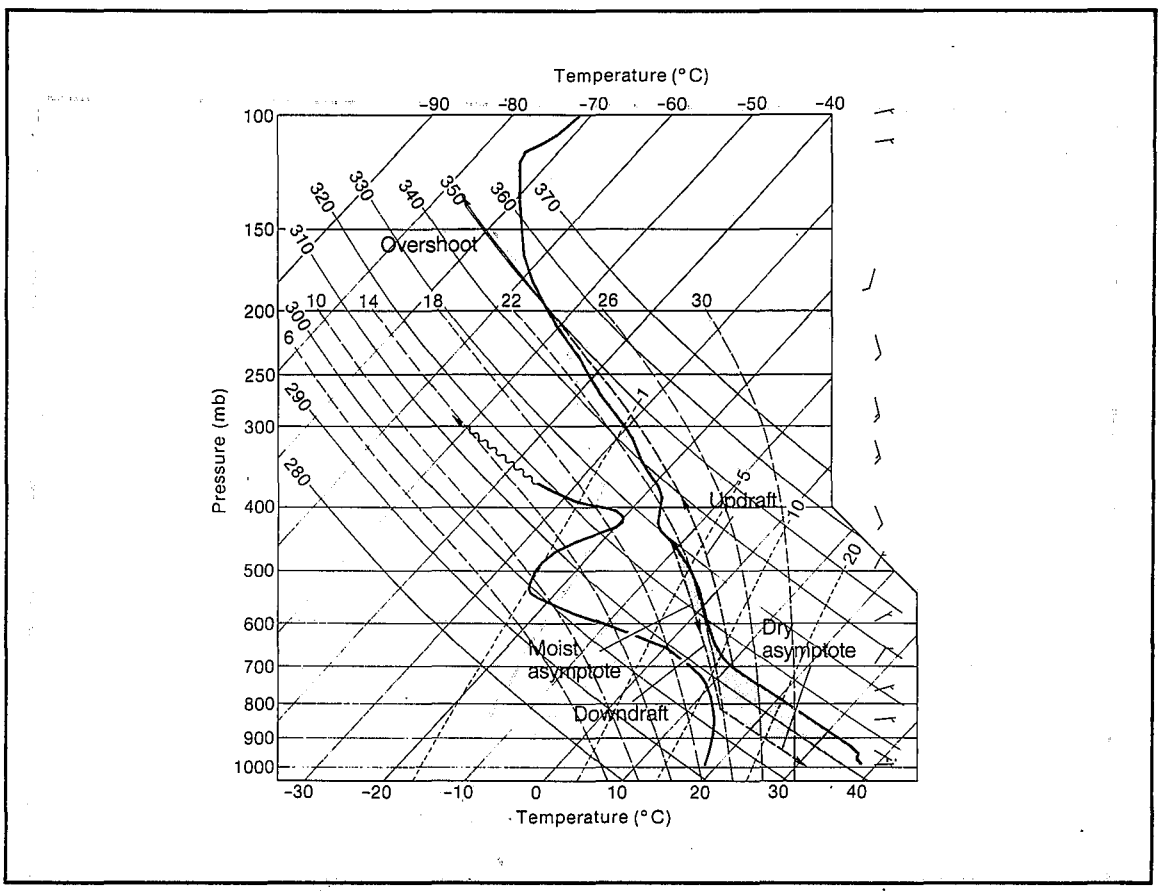

FIGURE 7
RECONSTRUCTED SOUNDING FOR DALLAS-FORT WORTH INTERNATIONAL AIRPORT FOR A TIME WHEN A MICROBURST-RELATED ACCIDENT HAPPENED (CARACENA et al, 1986)

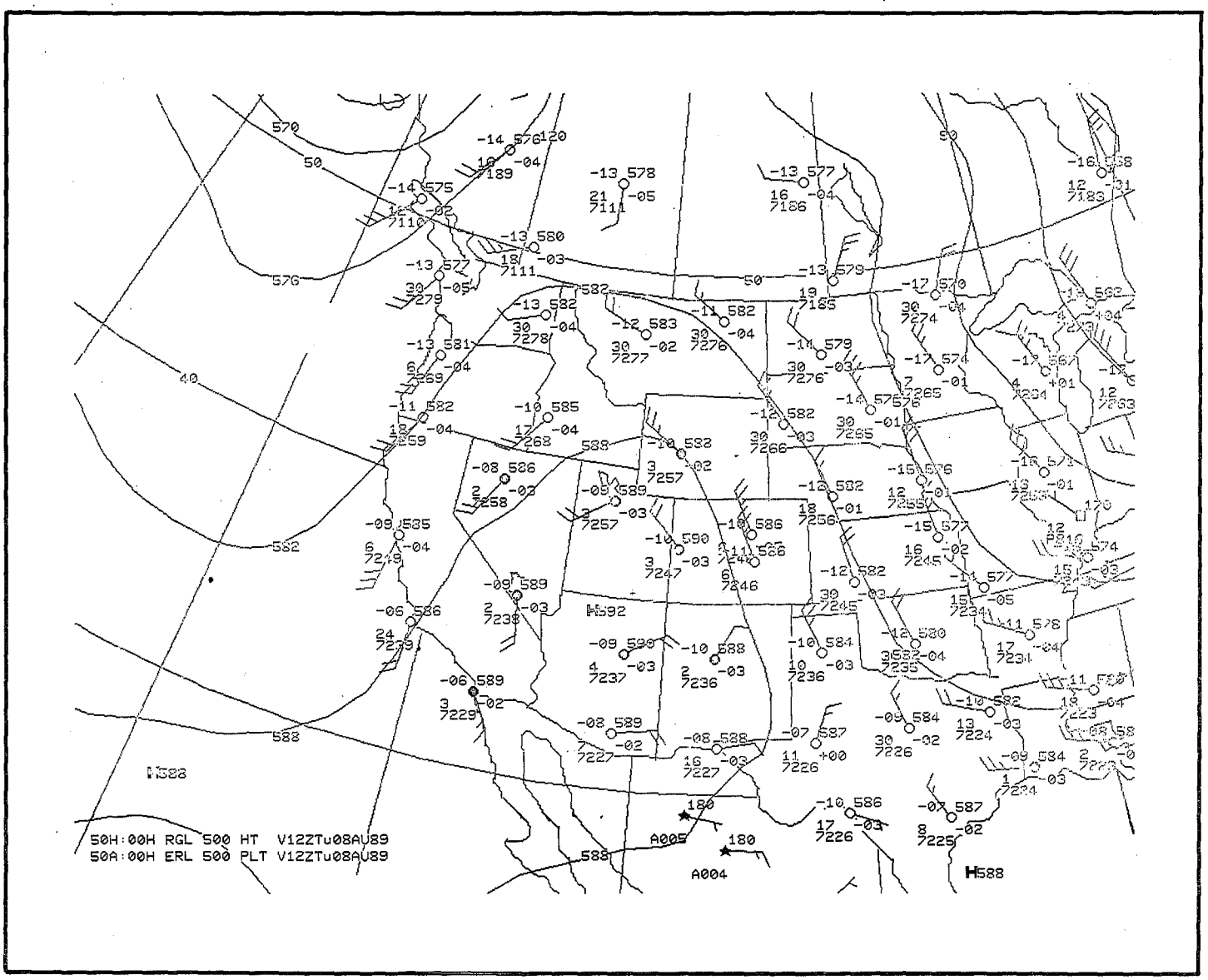

FIGURE 8
500-mb DATA PLT WITH CONTOUR ANALYSIS VALID AT 1200 UTC AUGUST 8, 1989

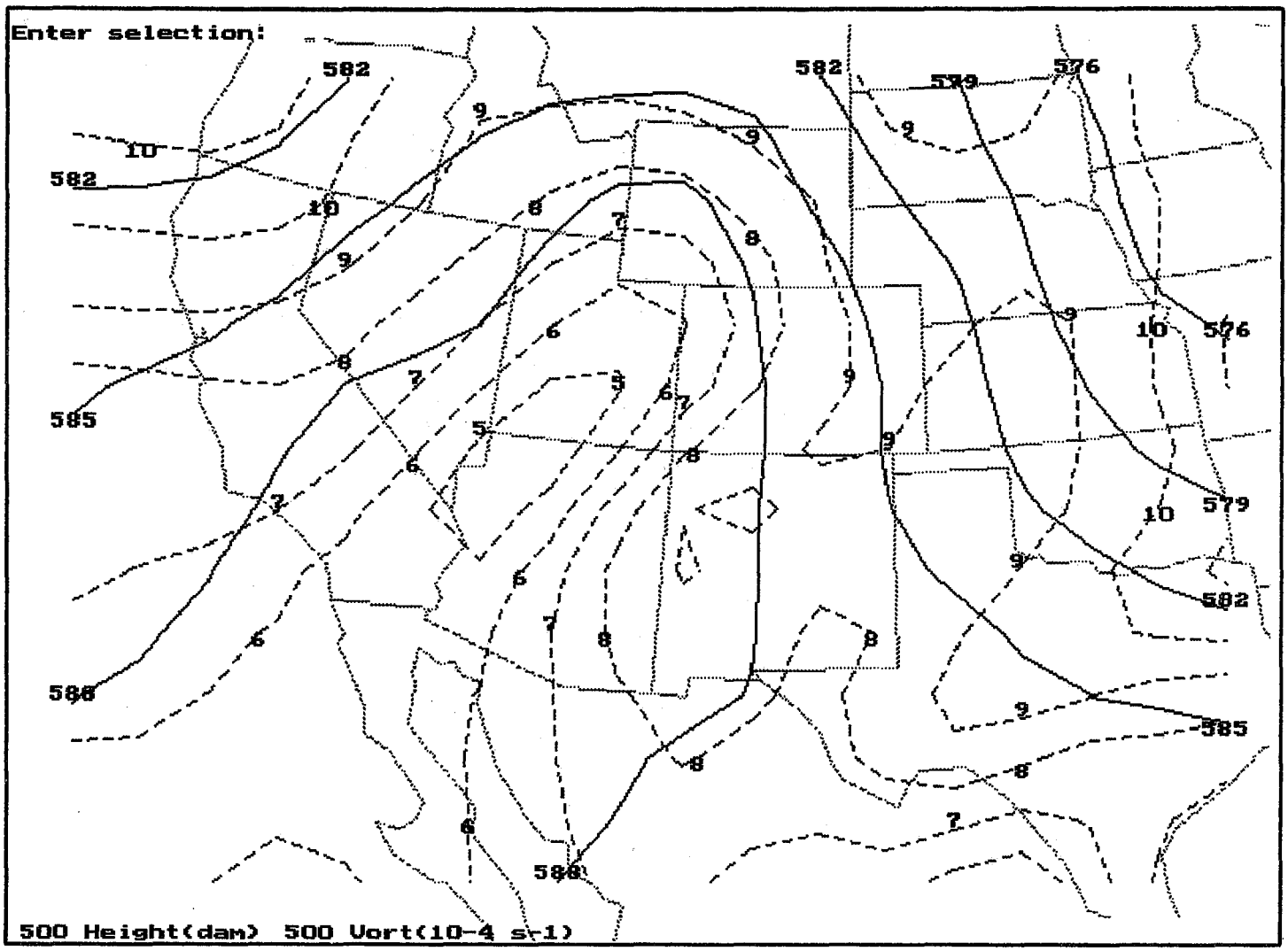

FIGURE 9
500-mb CONTOURED VORTICITY
ANALYSIS VALID AT 1200 UTC
(THE SOLID LINES ARE HEIGHT CONTOURS;
THE DASHED LINES REPRESENT VORTICITY ISOPLETHS)
AUGUST 8, 1989

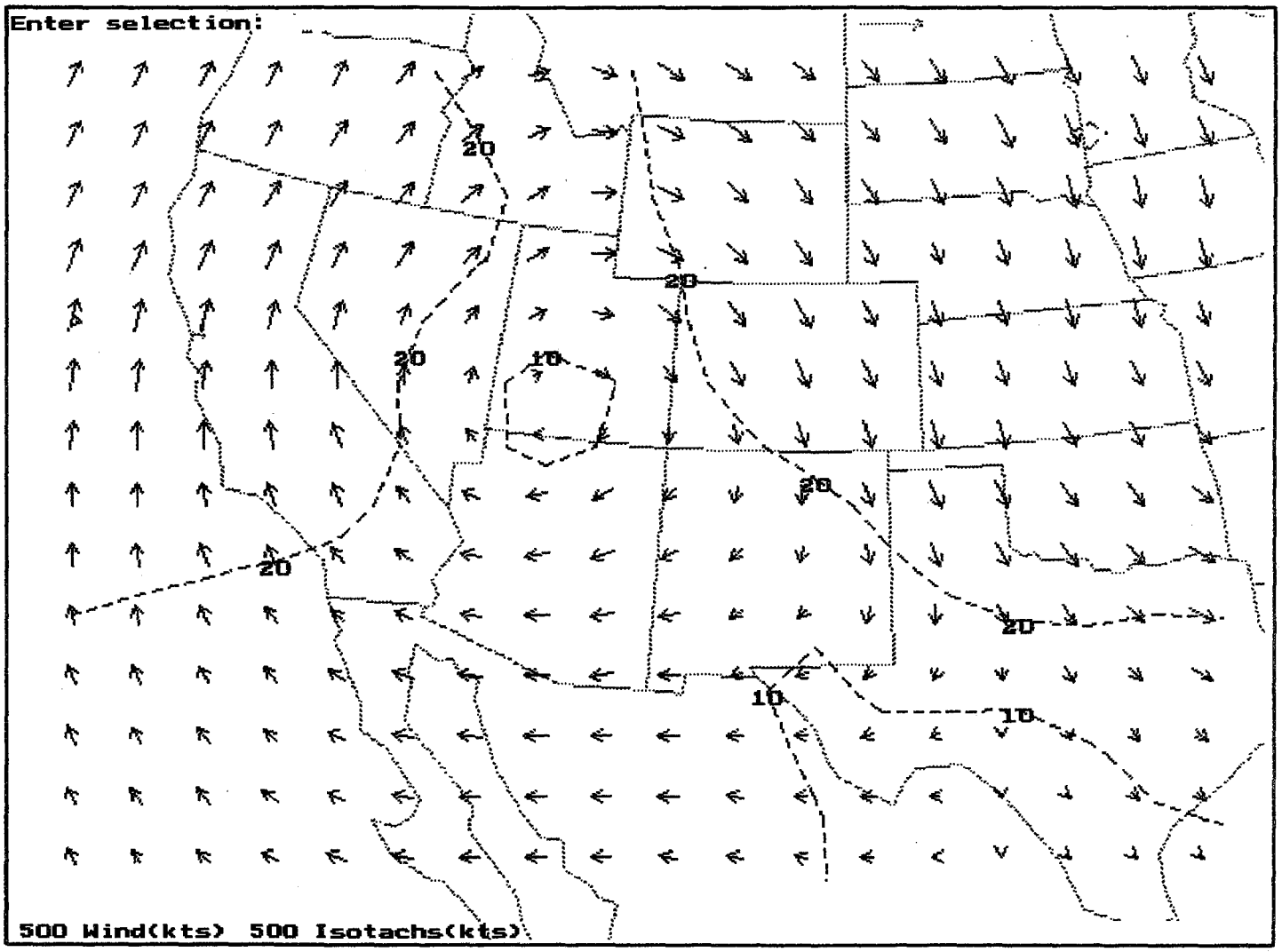

FIGURE 10
500-mb WIND FIELD ANALYSIS VALID AT 1200 UTC
AUGUST 8, 1989

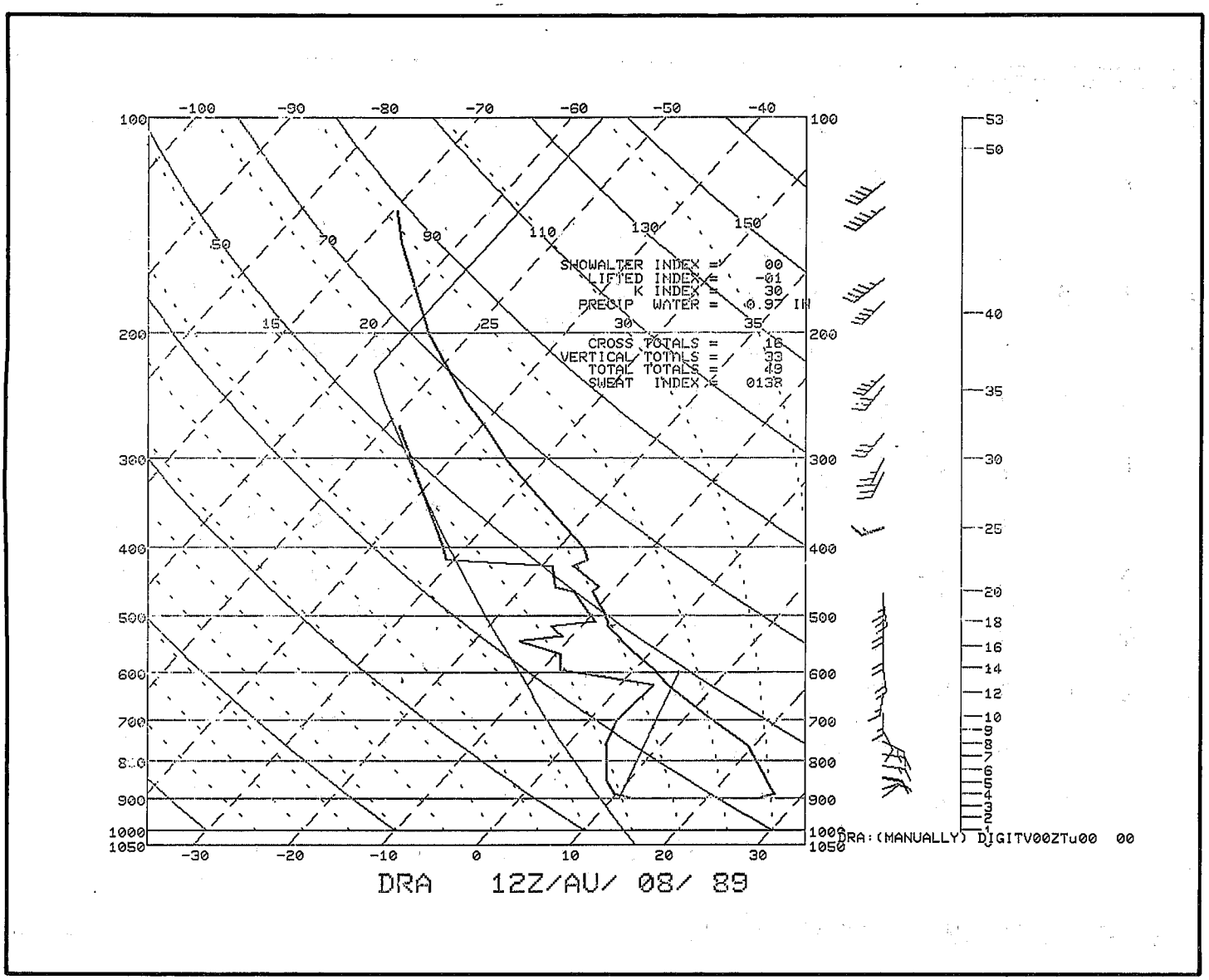

FIGURE 11
DRA SOUNDING VALID AT 1200 UTC
AUGUST 8, 1989

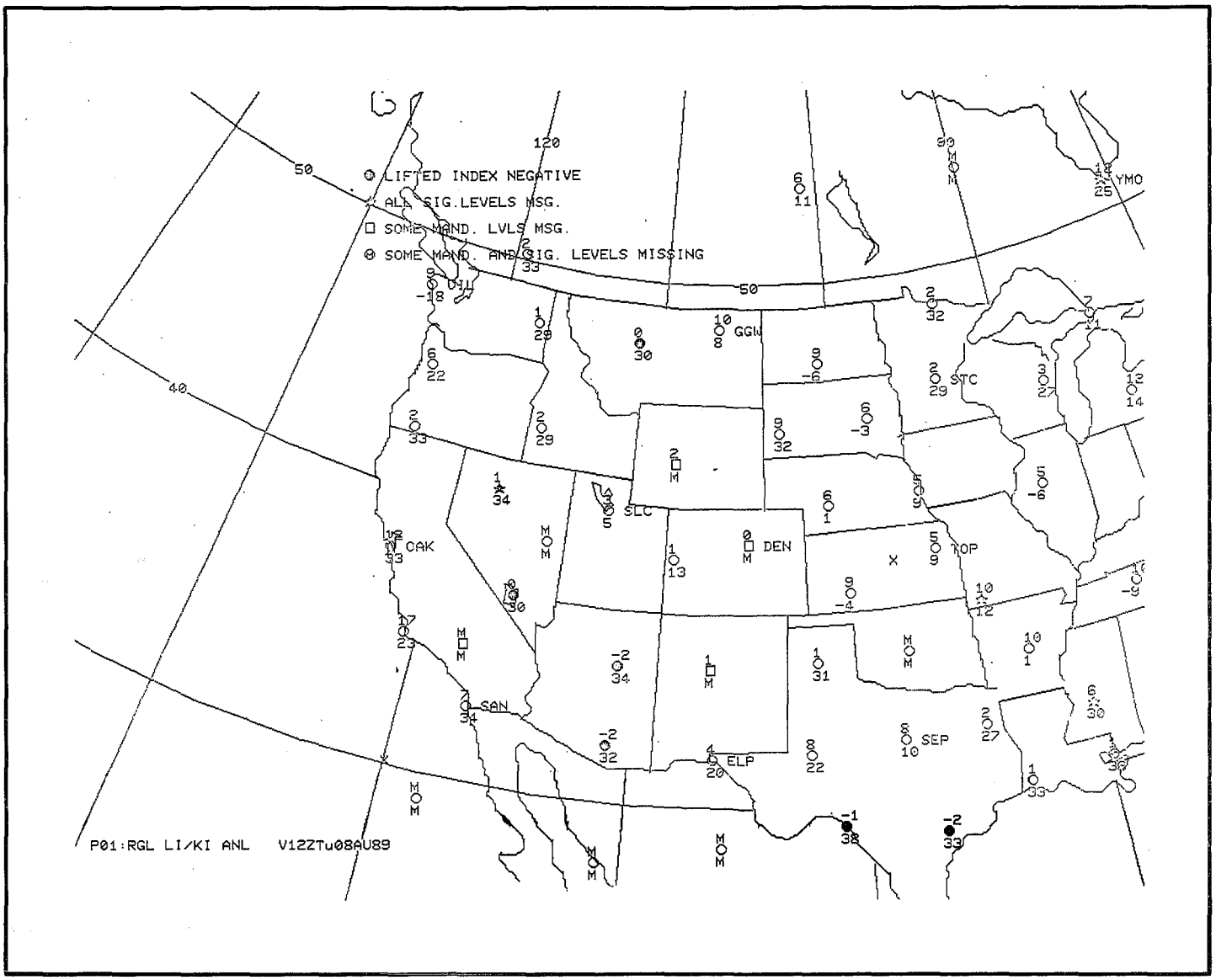

FIGURE 12
ANALYSIS OF THE LIFT INDEX (TOP NUMBER) AND K-INDEX (BOTTOM NUMBER) VALID AT 1200 UTC AUGUST 8, 1989

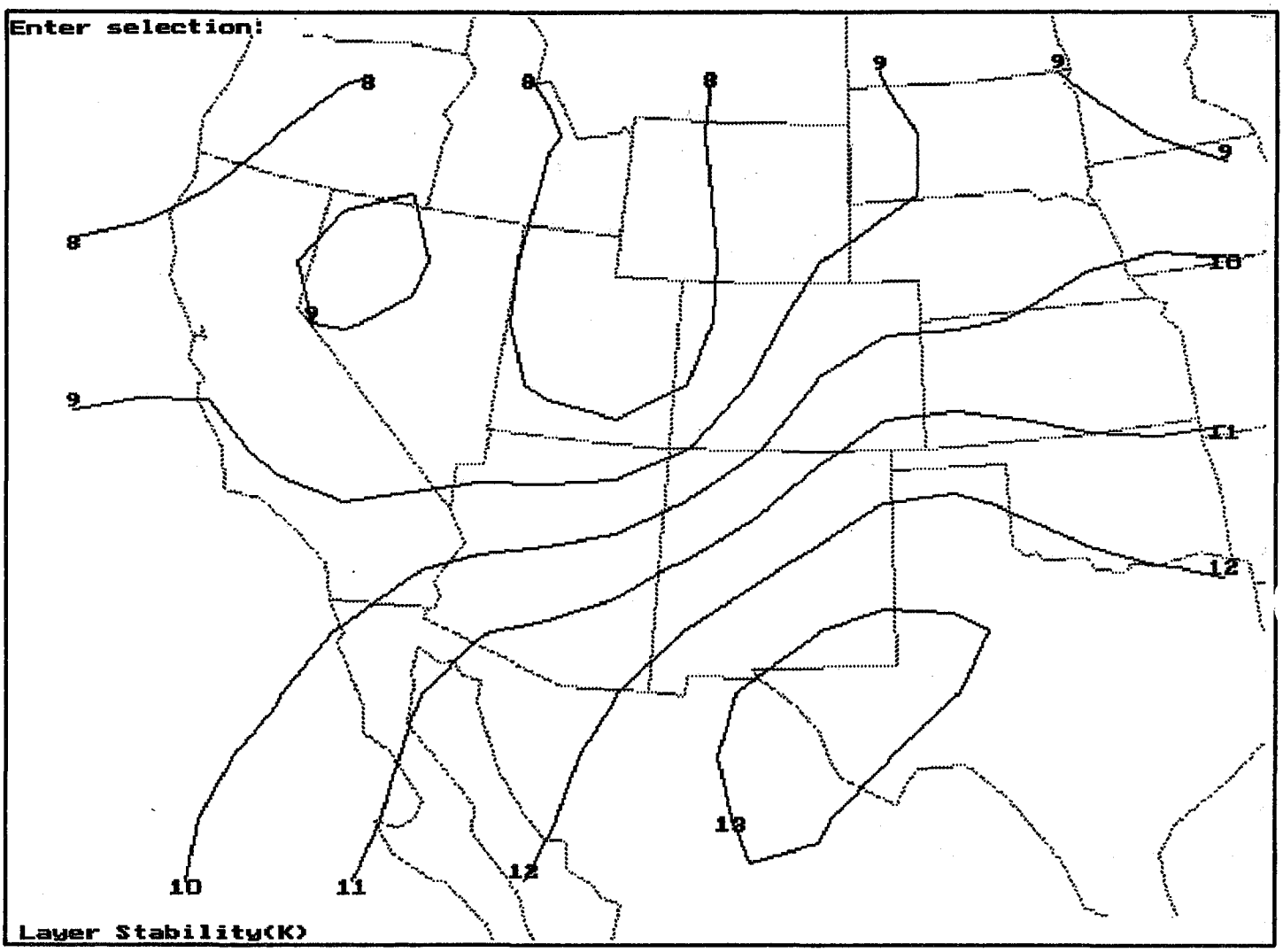

FIGURE 13
ANALYSIS OF THE LAYER STABILITY VALID AT 1200 UTC
AUGUST 8, 1989

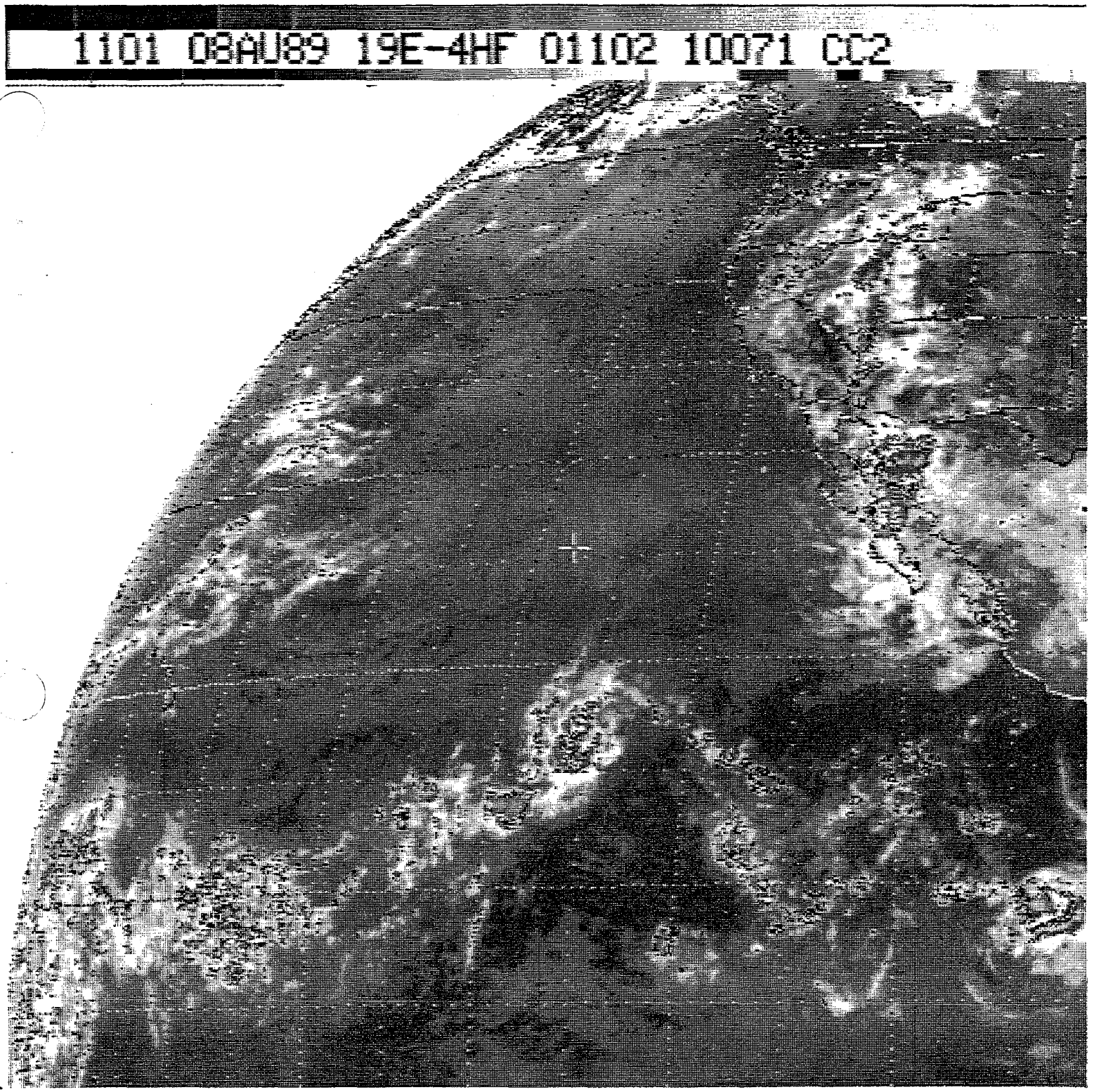

FIGURE 14
ENHANCED IR SATELLITE IMAGERY VALID AT 1200 UTC
AUGUST 8, 1989

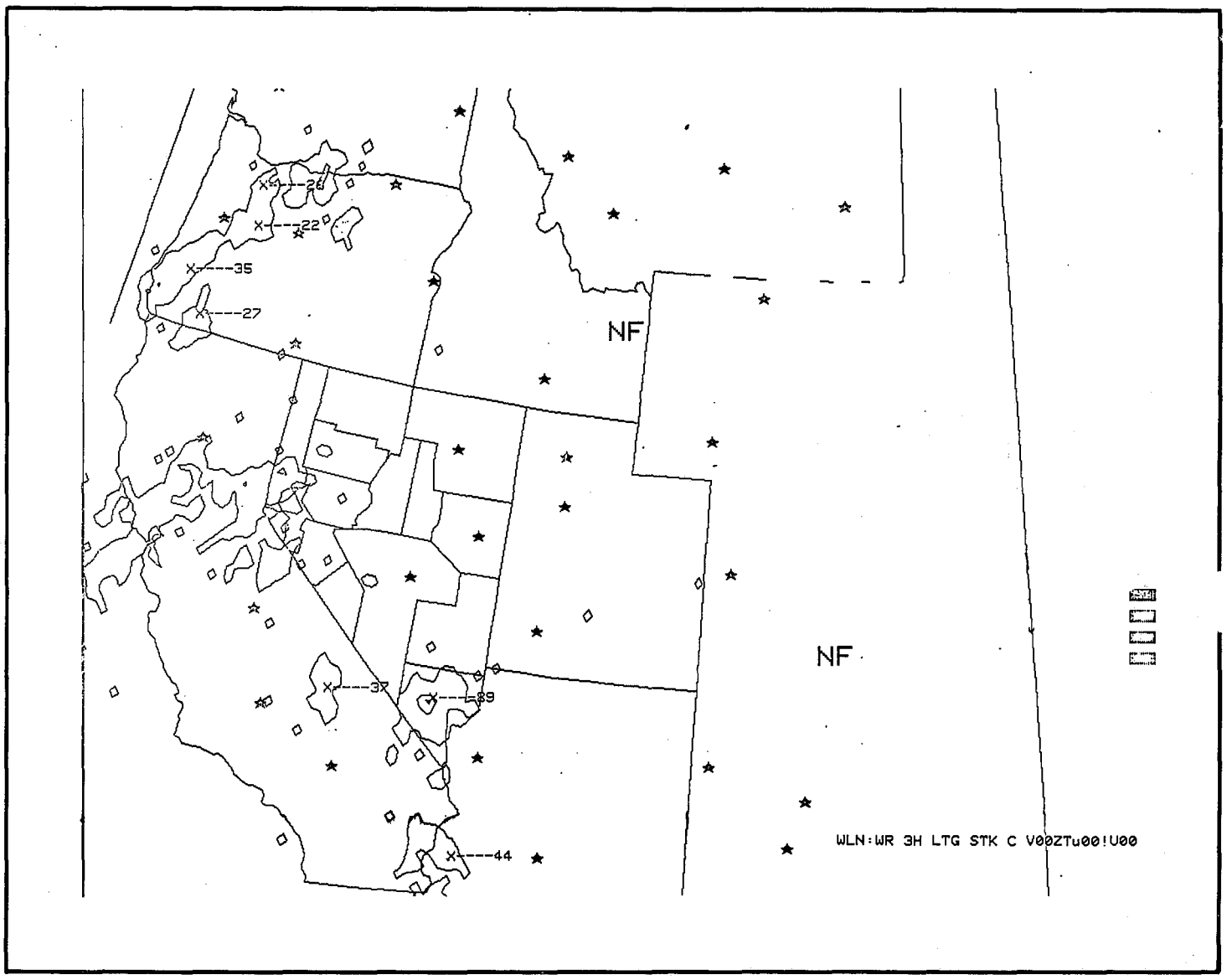

FIGURE 15
ANALYSIS OF THE CG LIGHTNING DATA VALID AT 1215 UTC
AUGUST 8, 1989

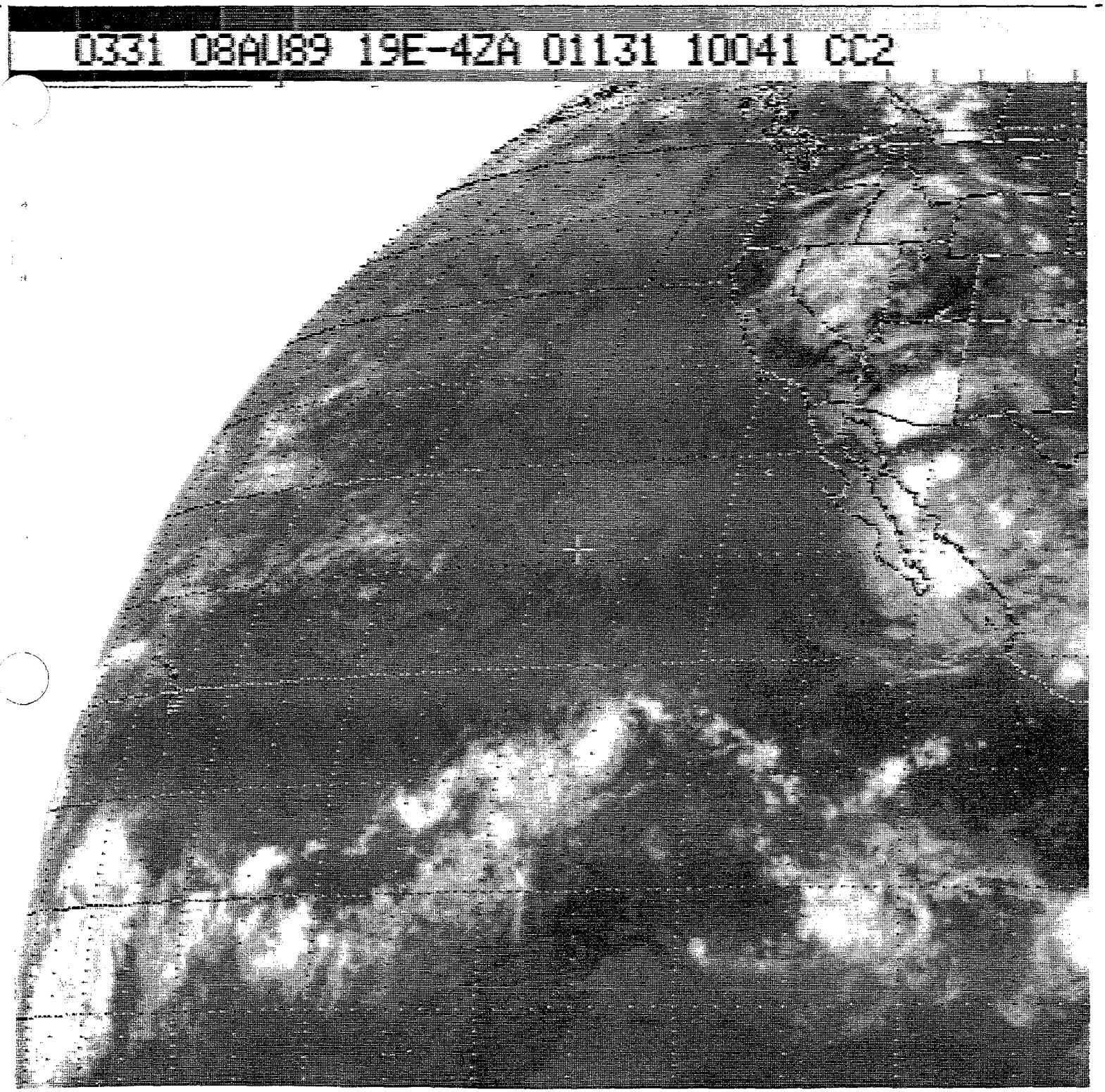

FIGURE 16
IR SATELLITE IMAGERY VALID AT 0331 UTC
AUGUST 8, 1989

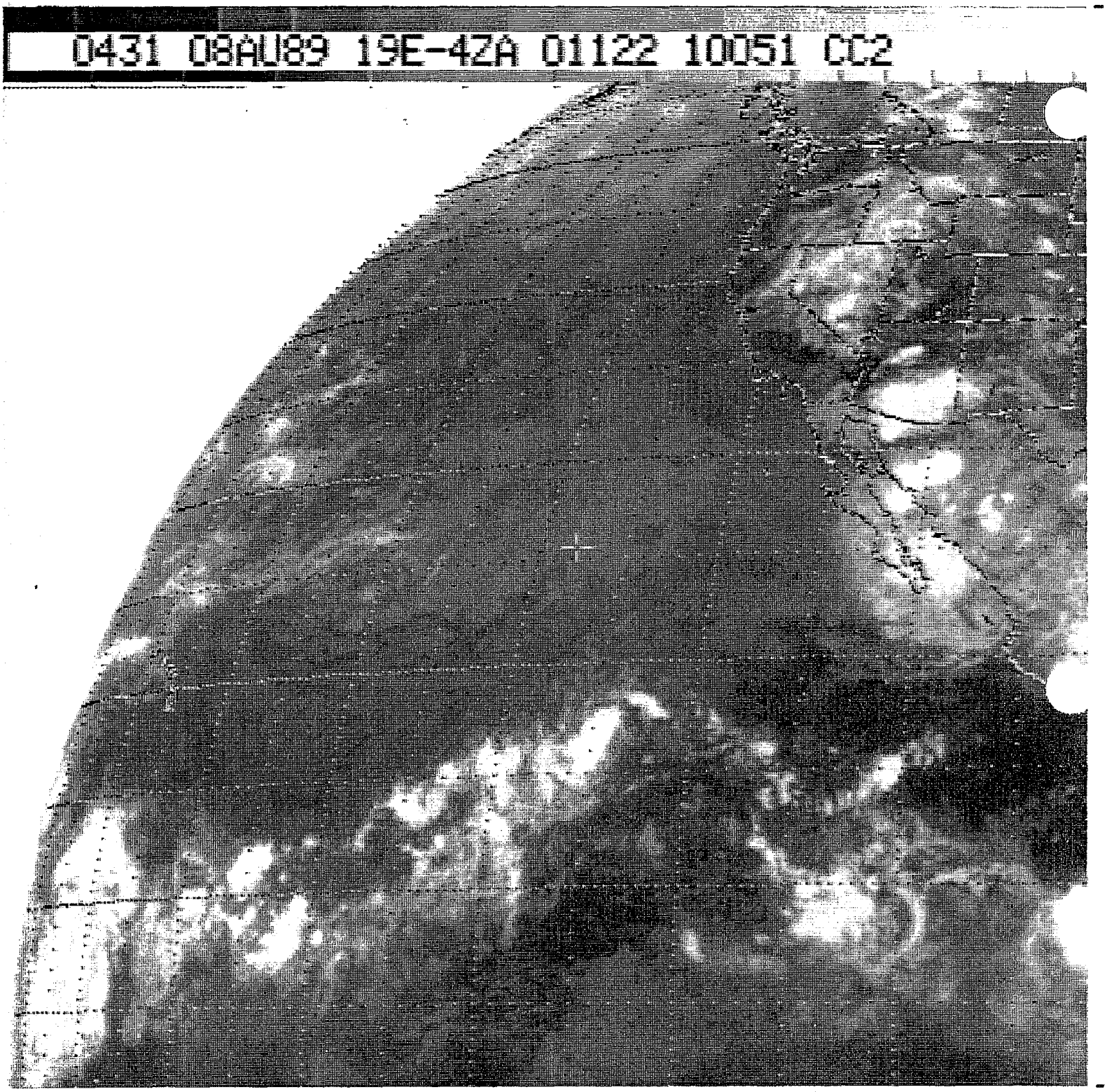

FIGURE 17
IR SATELLITE IMAGERY VALID AT 0431 UTC
AUGUST 8, 1989

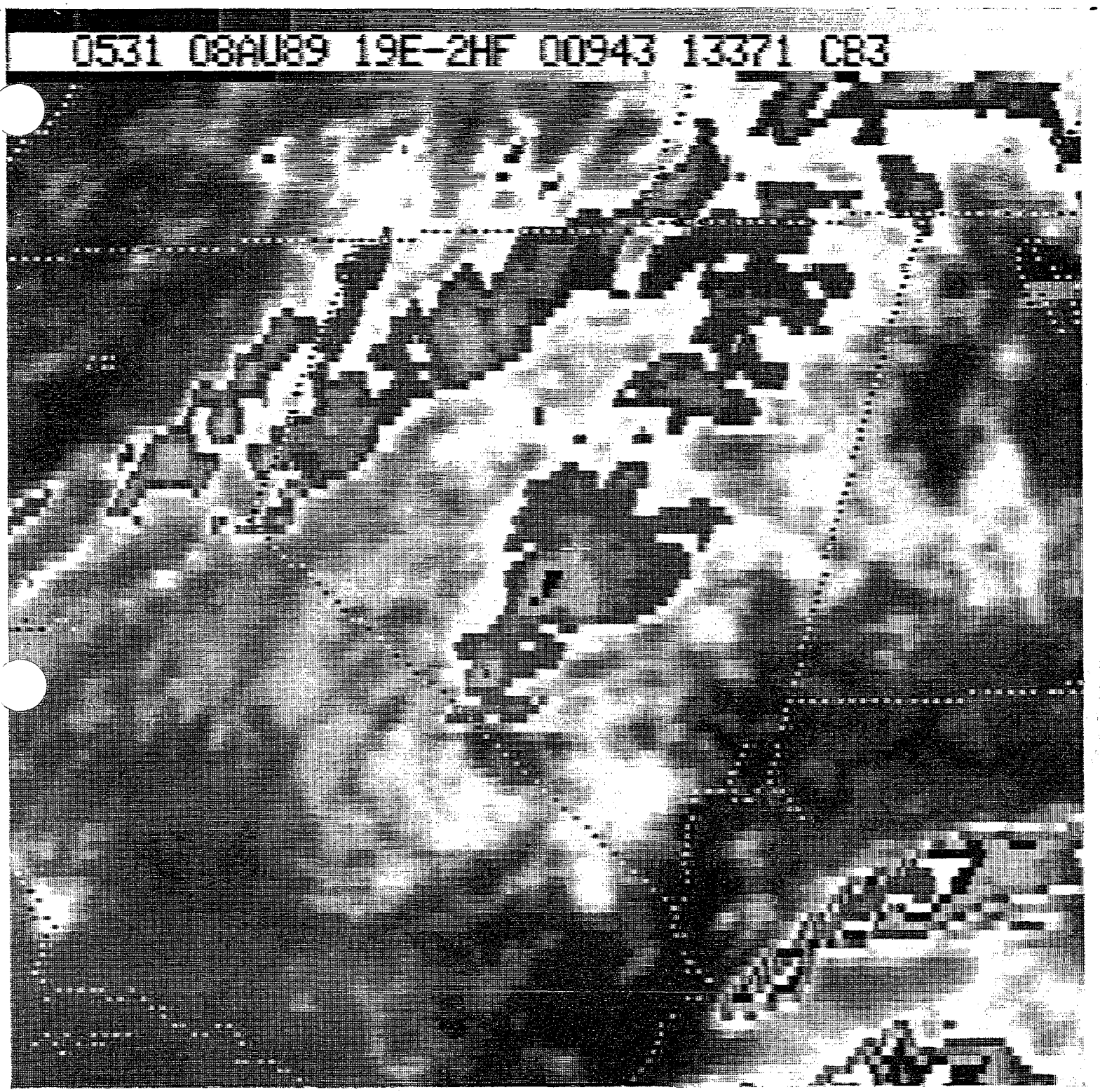

FIGURE 18
IR SATELLITE IMAGERY VALID AT 0531 UTC
AUGUST 8, 1989

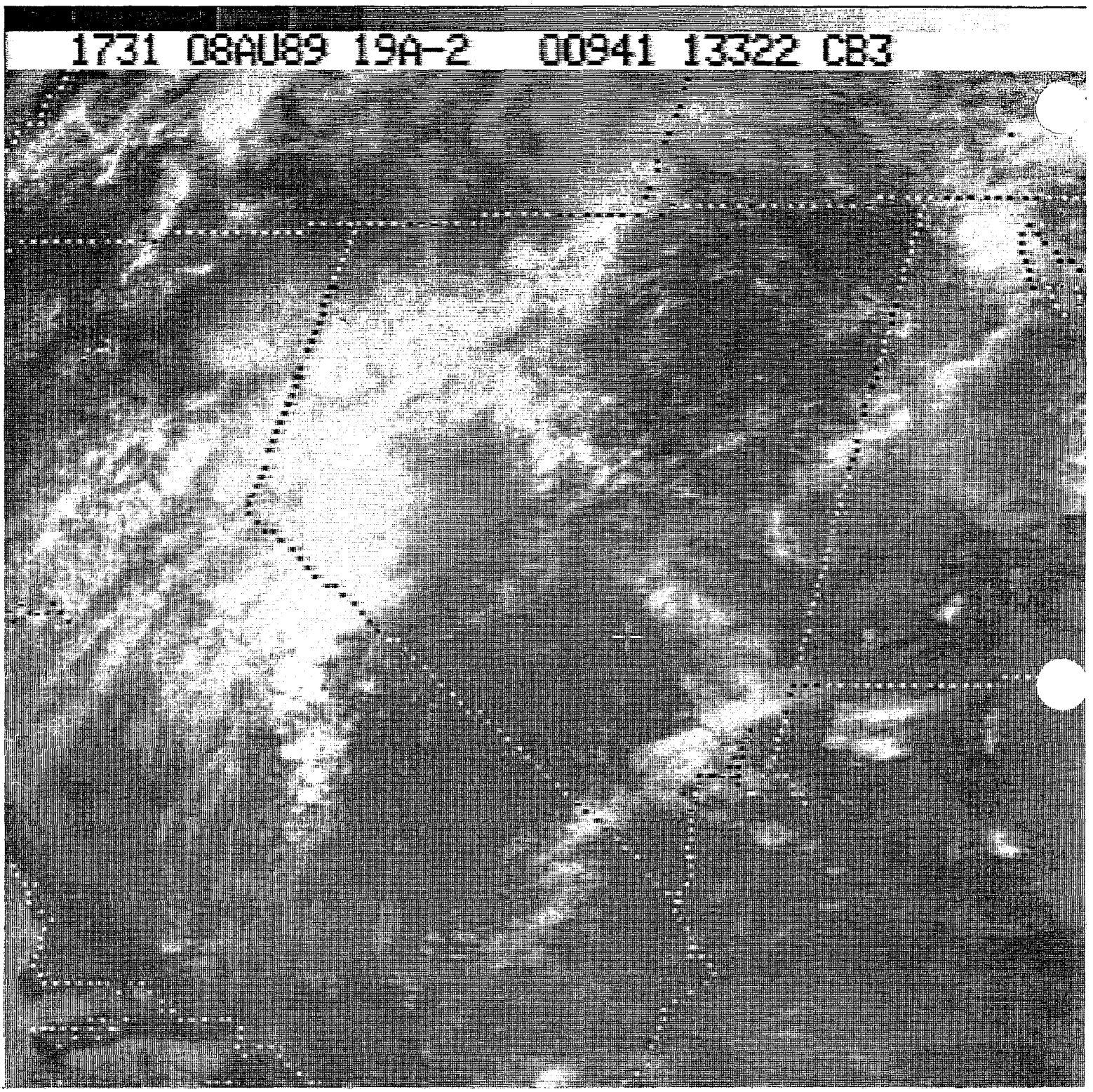

FIGURE 19
VISIBLE SATELLITE IMAGERY VALID AT 1731 UTC
AUGUST 8, 1989

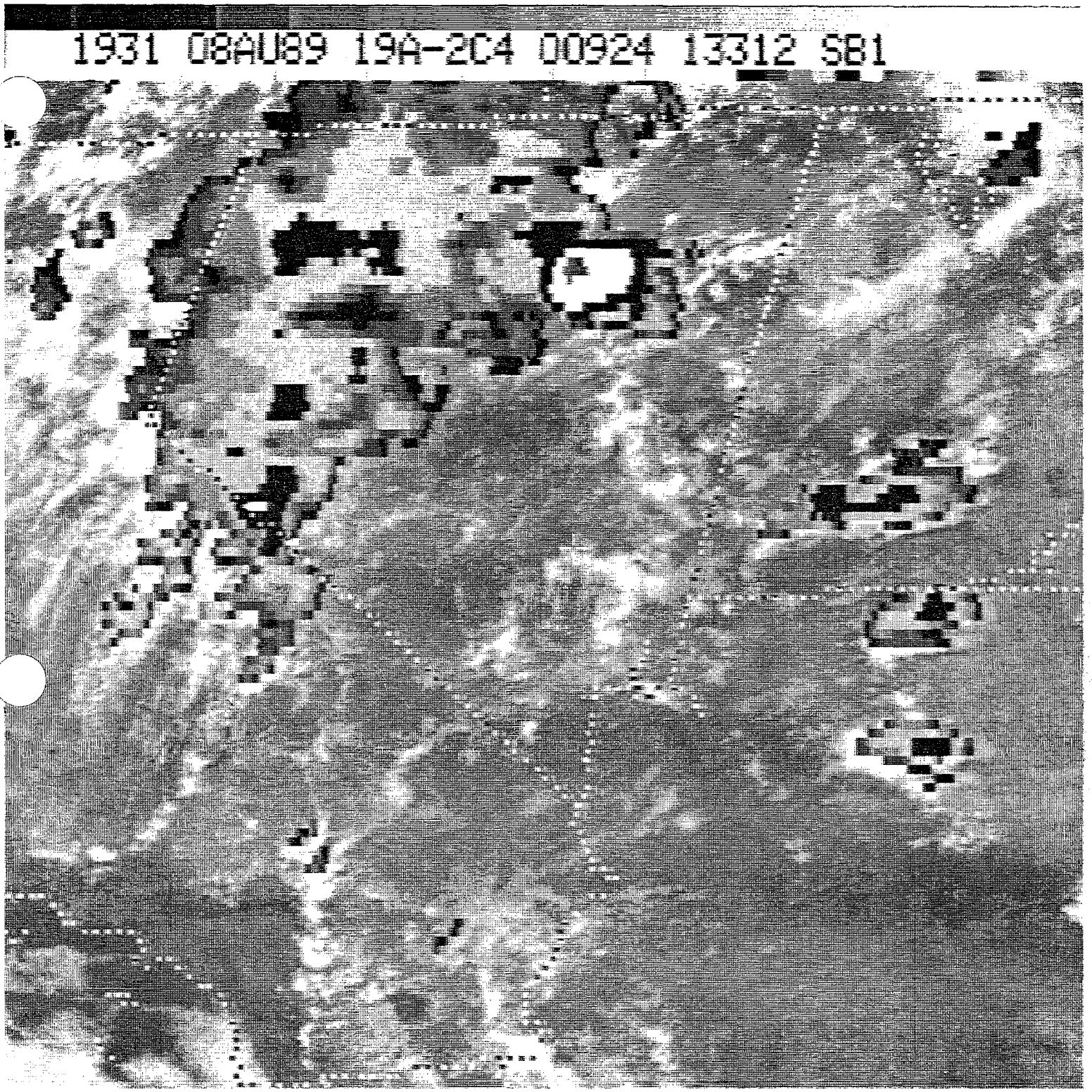

FIGURE 20
ENHANCED VISIBLE SATELLITE IMAGERY VALID AT 1931 UTC
AUGUST 8, 1989

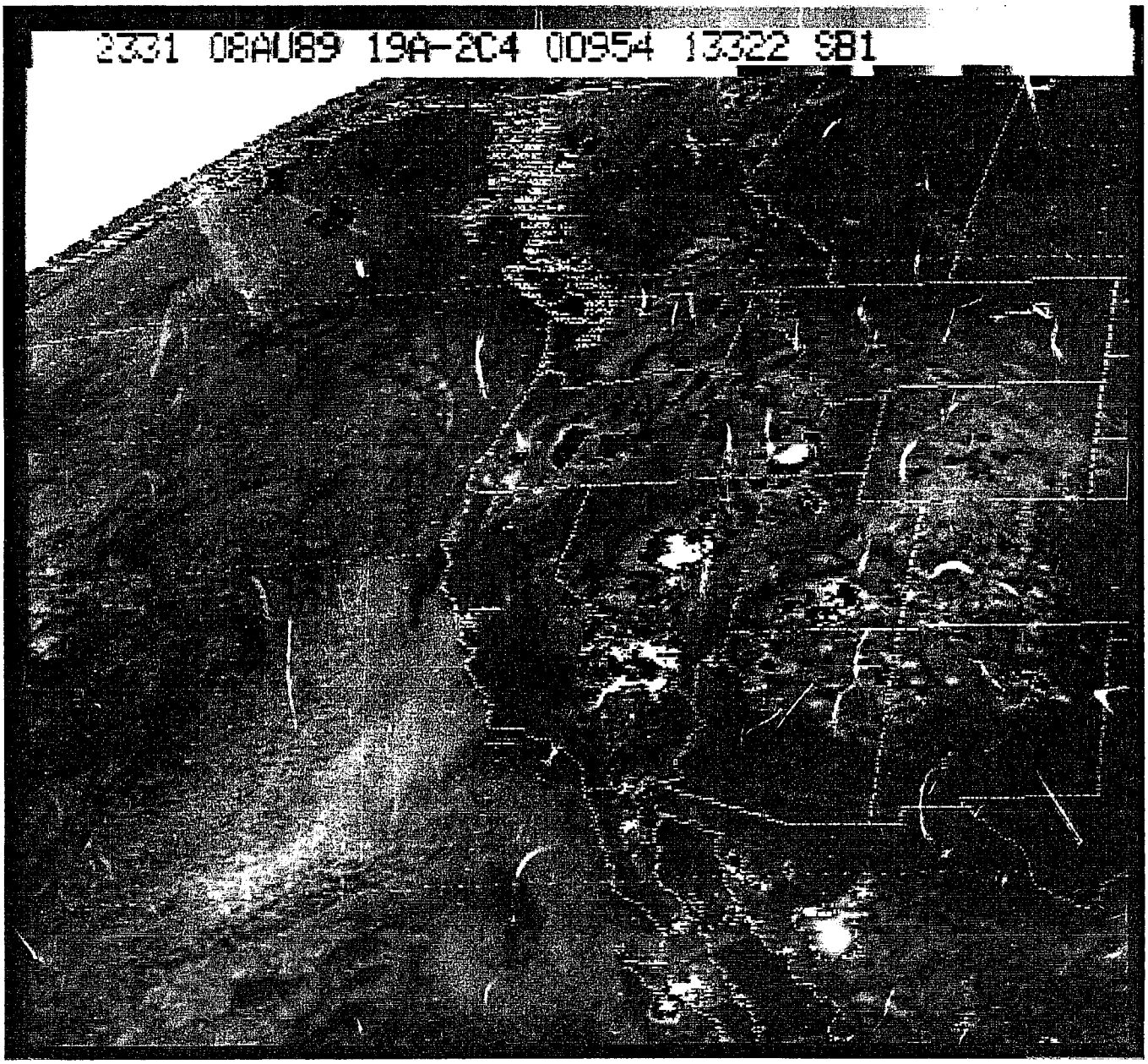

FIGURE 21
ENHANCED VISIBLE SAT IMAGERY VALID AT 2331 UTC
AUGUST 8, 1989

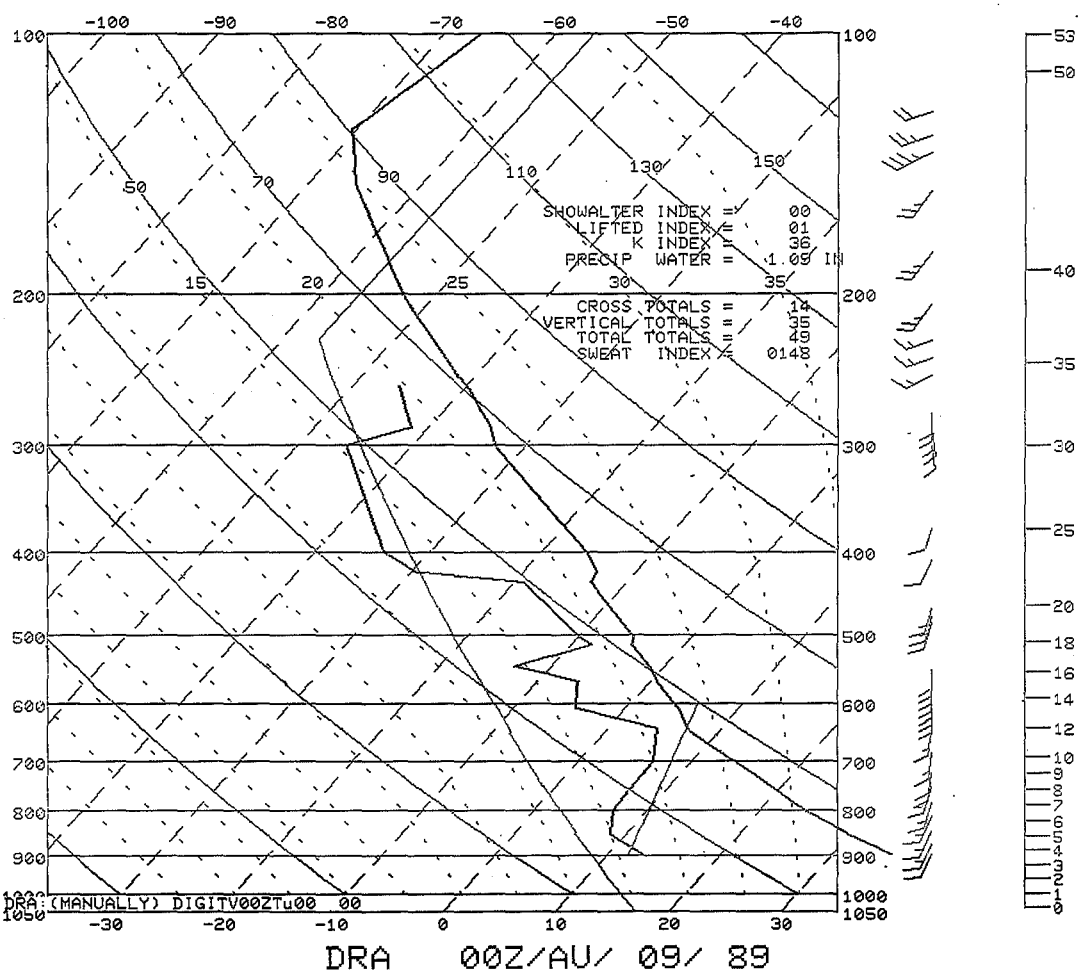

FIGURE 22
DRA SOUNDING VALID AT 0000 UTC
AUGUST 9, 1989

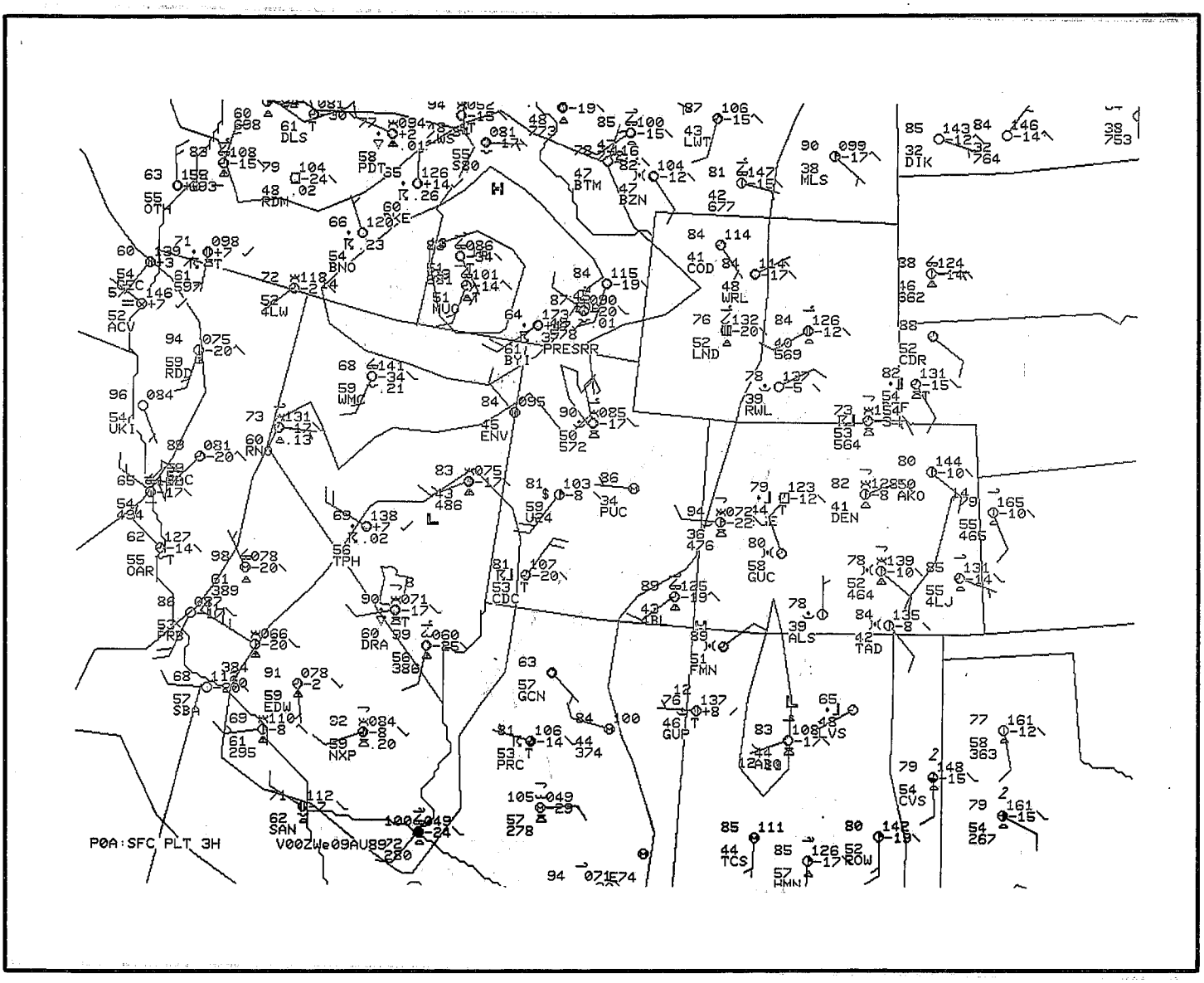

FIGURE 23
SURFACE PRESSURE ANALYSIS (4 mb INTERVAL)
AND DATA PLOT VALID AT 0000 UTC
AUGUST 9, 1989

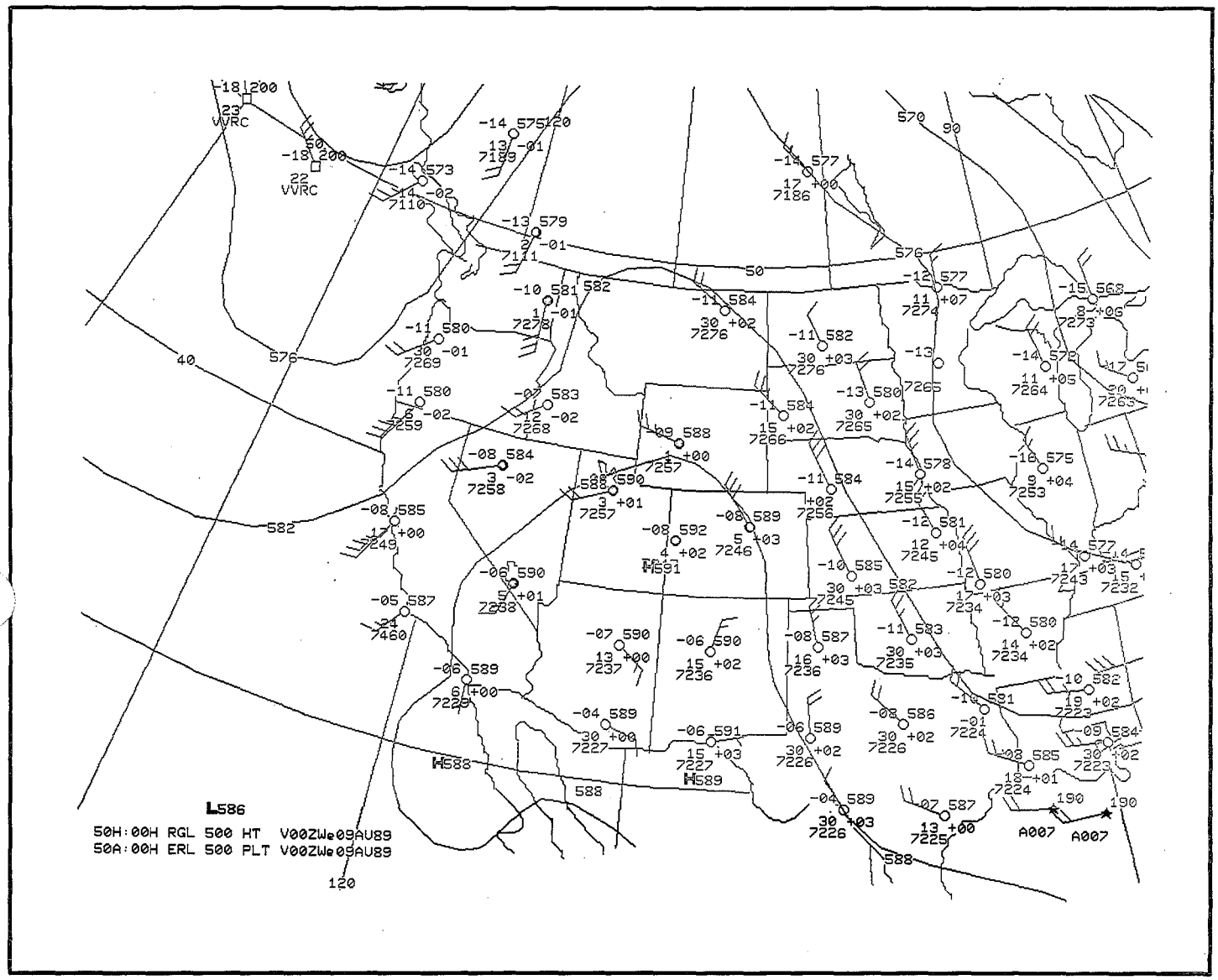

FIGURE 24
500-mb CONTOUR ANALYSIS AND
DATA PLOT VALID AT 0000 UTC
AUGUST 9, 1989

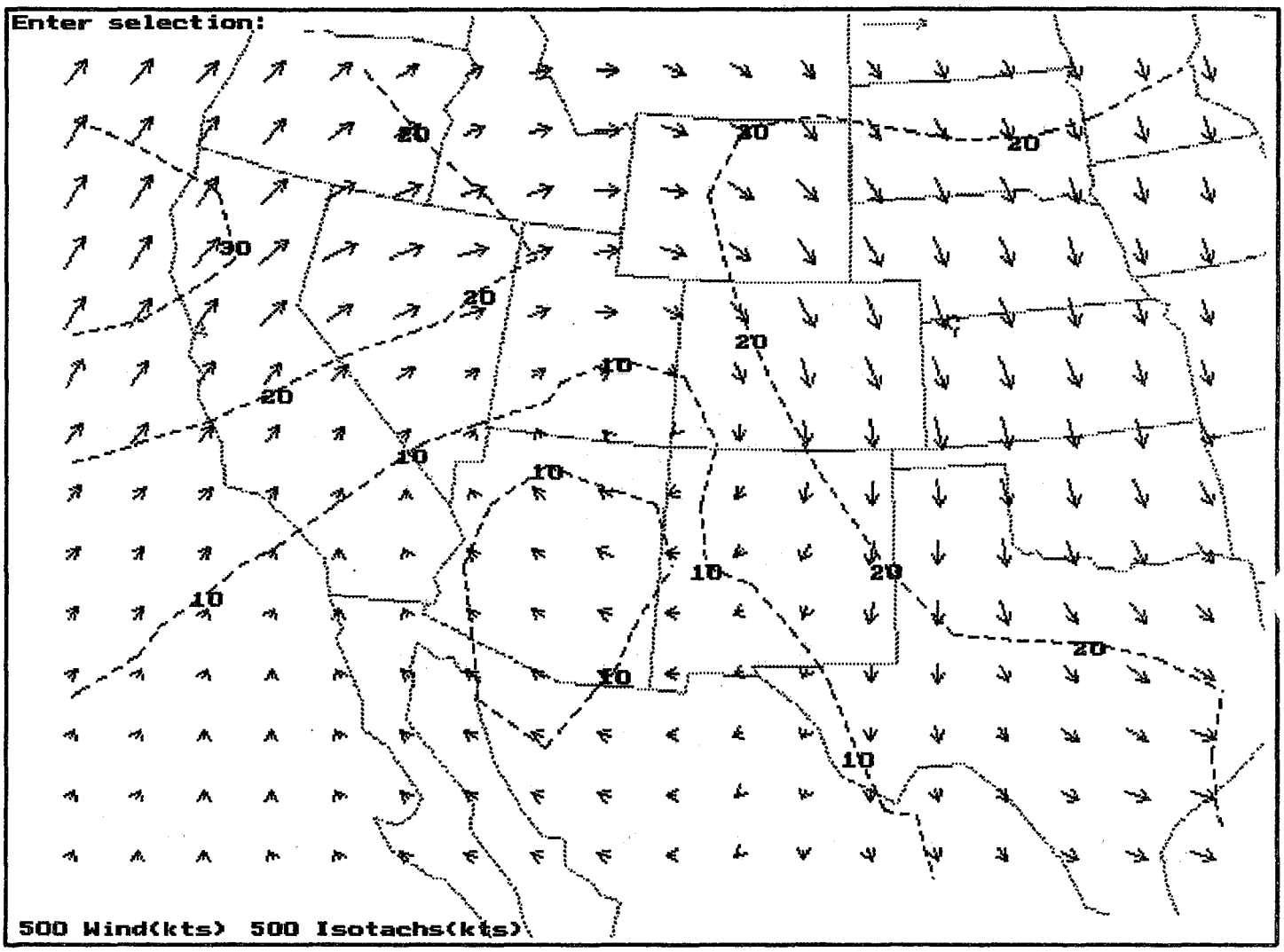

FIGURE 25
500-mb WIND FIELD ANALYSIS VALID AT 0000 UTC
AUGUST 9, 1989

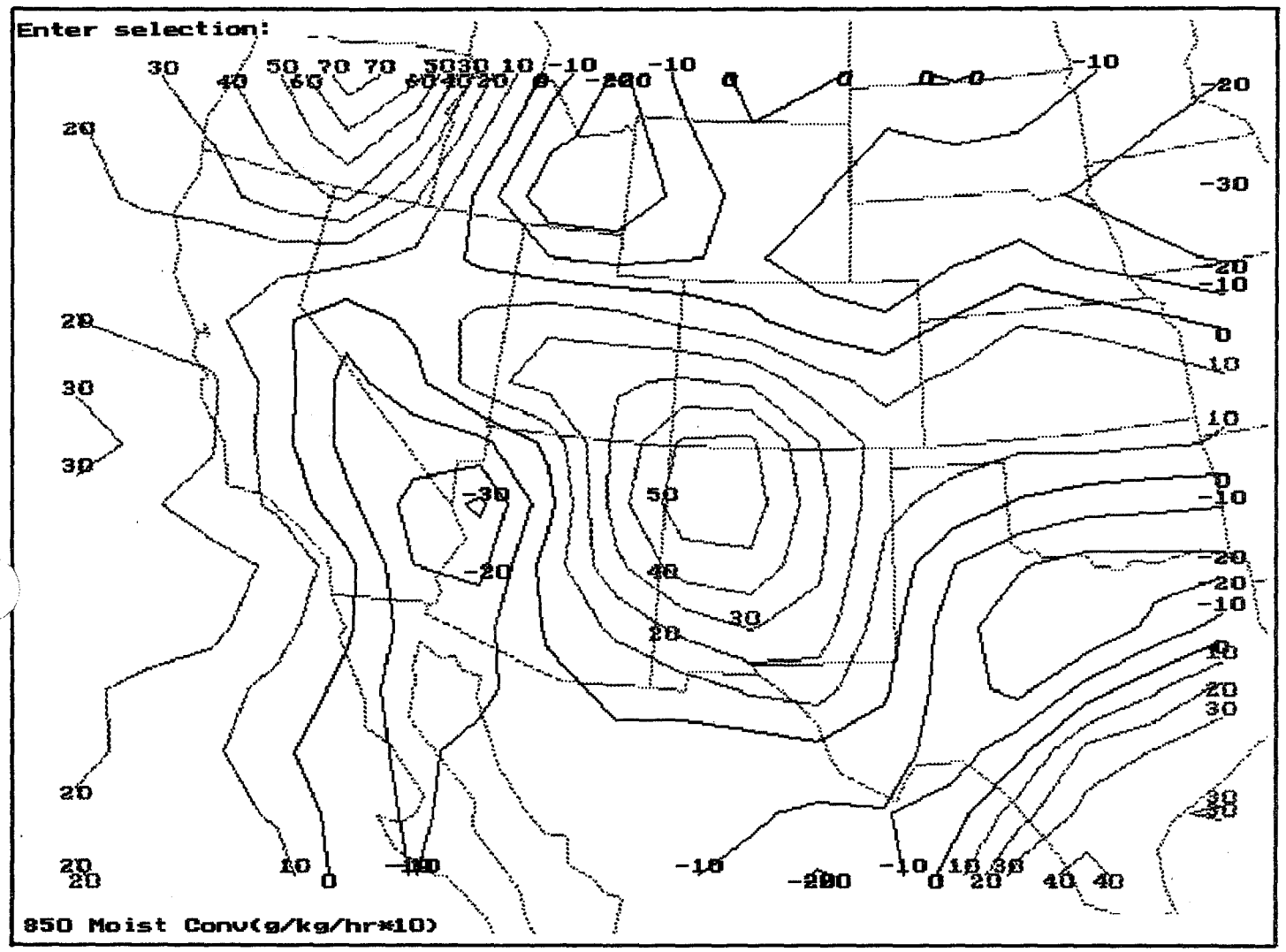

FIGURE 26
850-mb MOISTURE FLUX CONVERGENCE
ANALYSIS VALID AT 0000 UTC
AUGUST 9, 1989

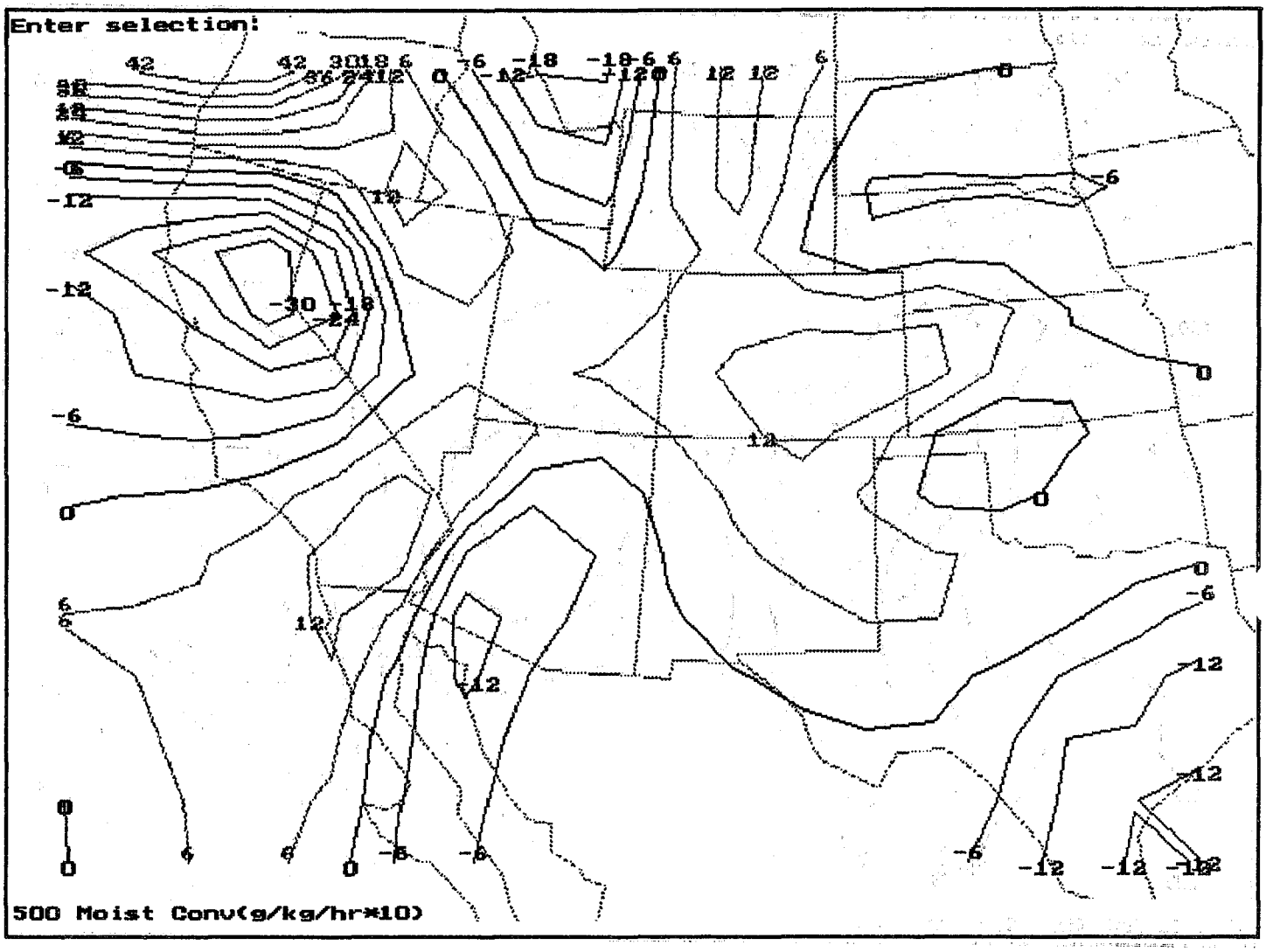

FIGURE 27
500-mb MOISTURE FLUX CONVERGENCE
ANALYSIS VALID AT 0000 UTC
AUGUST 9, 1989

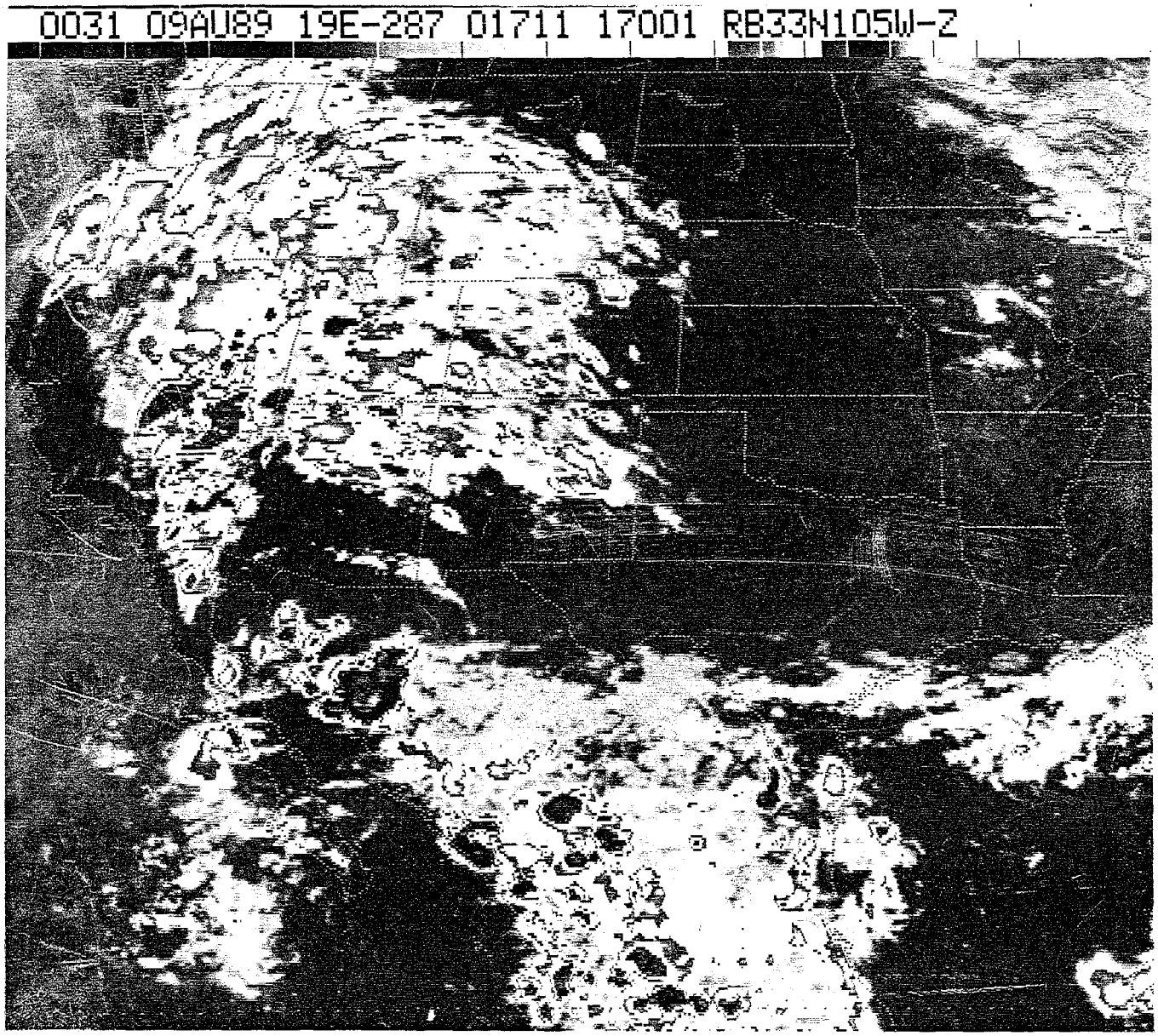

FIGURE 28
ENHANCED IR SATELLITE IMAGERY VALID AT 0031 UTC
AUGUST 9, 1989

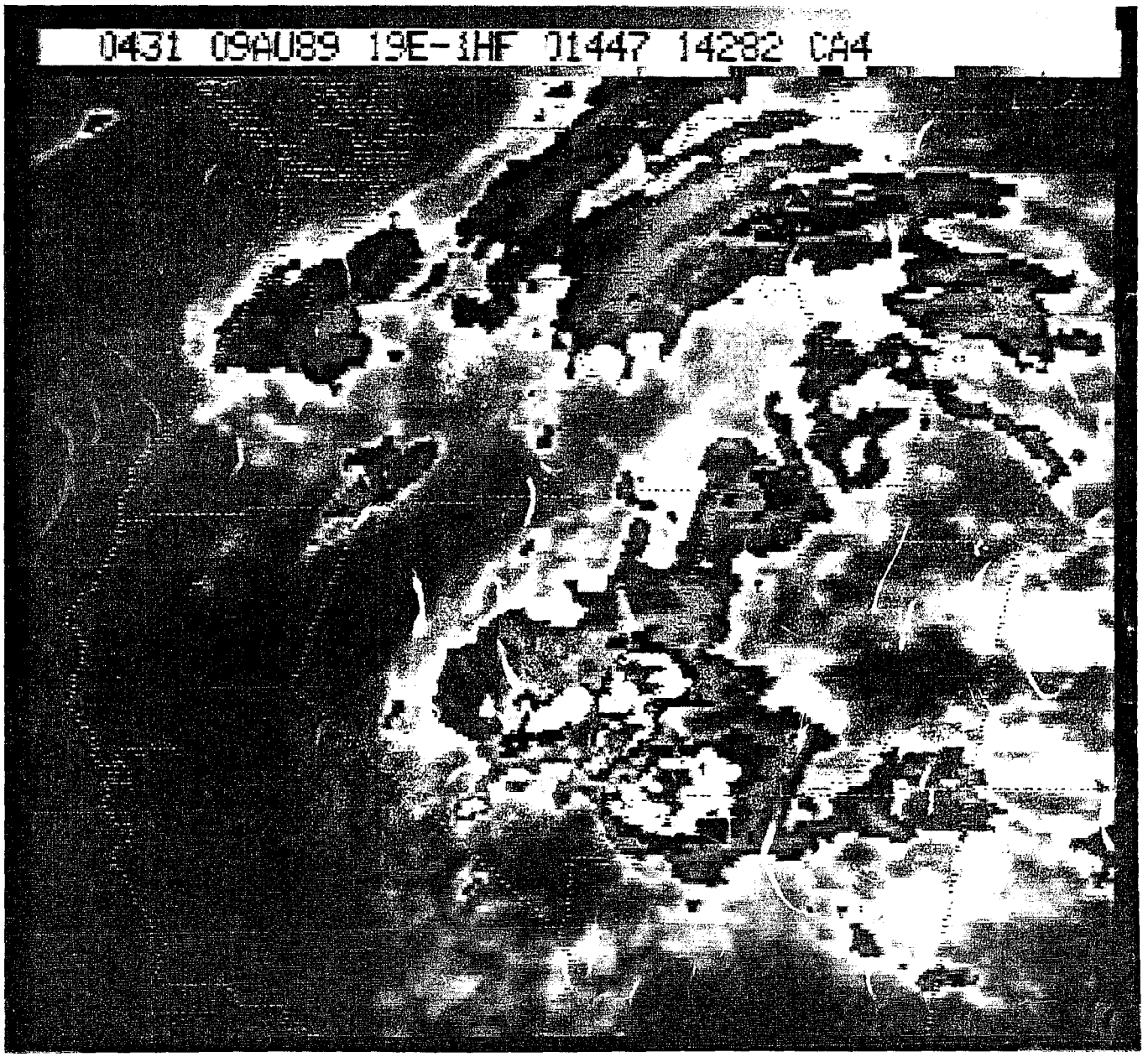

FIGURE 29
ENHANCED IR SATELLITE IMAGERY VALID AT 0431 UTC
AUGUST 9, 1989

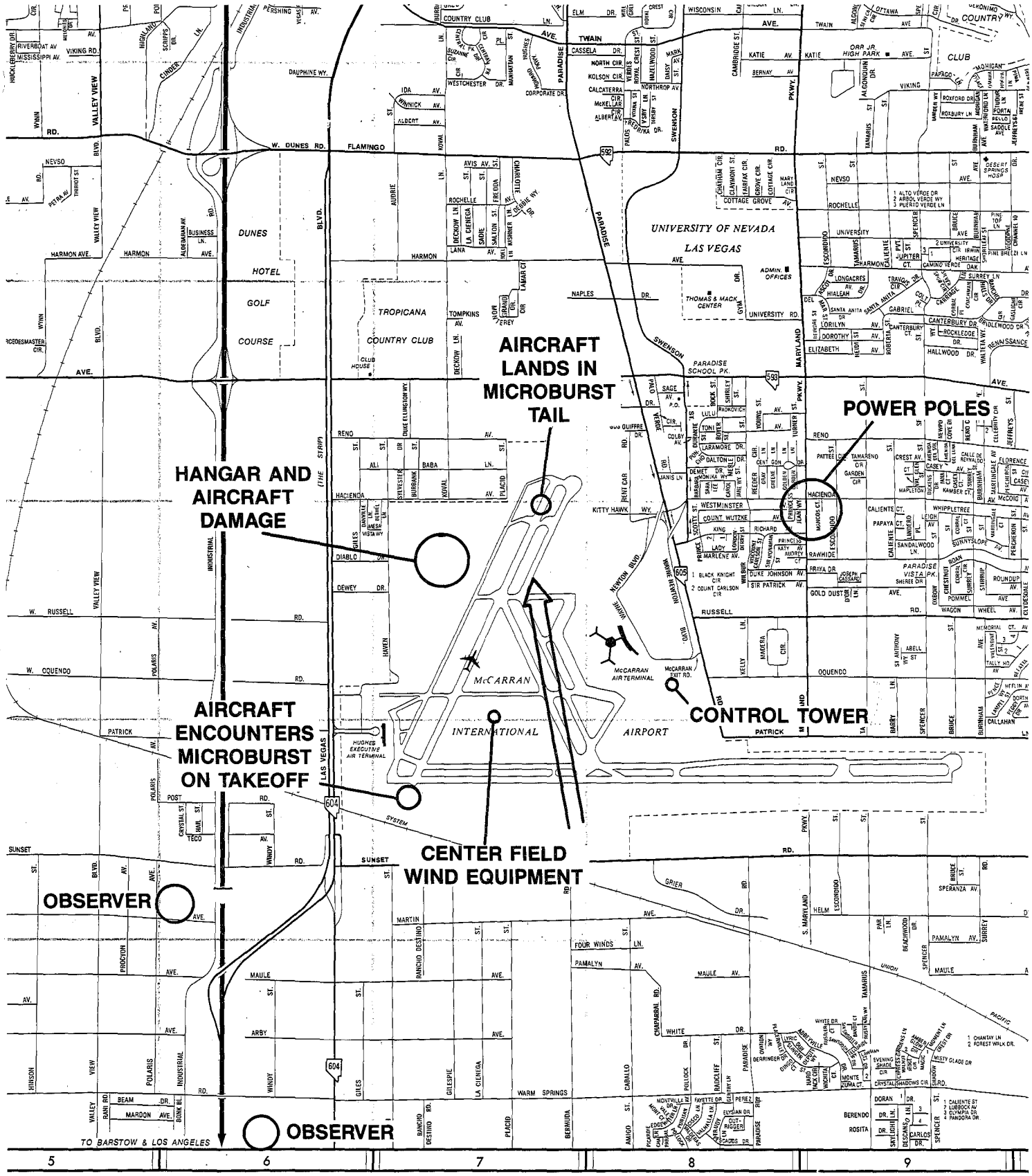

FIGURE 30
APPROXIMATE GROUND LOCATIONS OF DAMAGE IN THE McCARRAN AIRPORT VICINITY

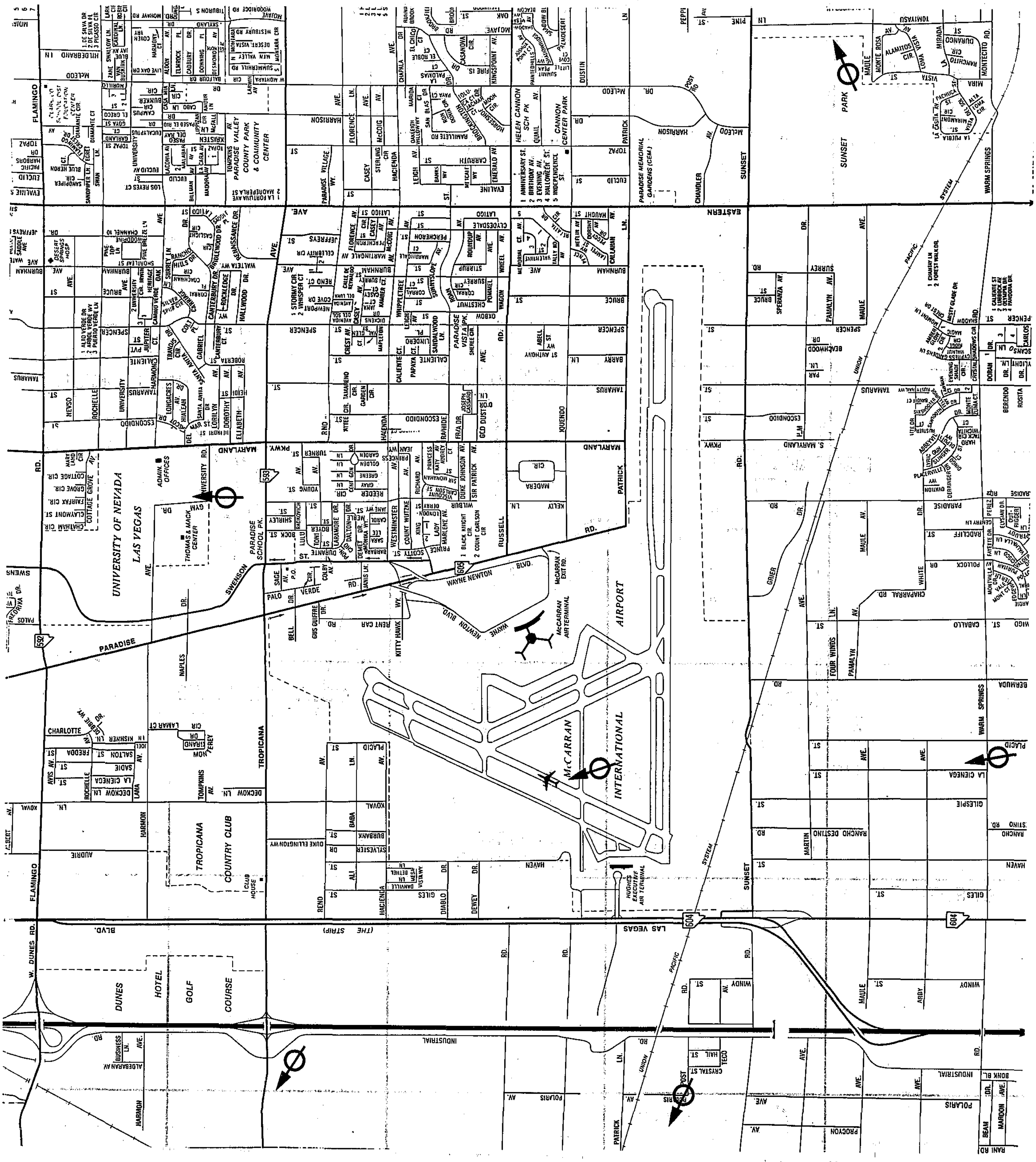

FIGURE 31
WIND DIRECTION FROM THE LLWAS
AT THE HEIGHT MICROBURST EVENT

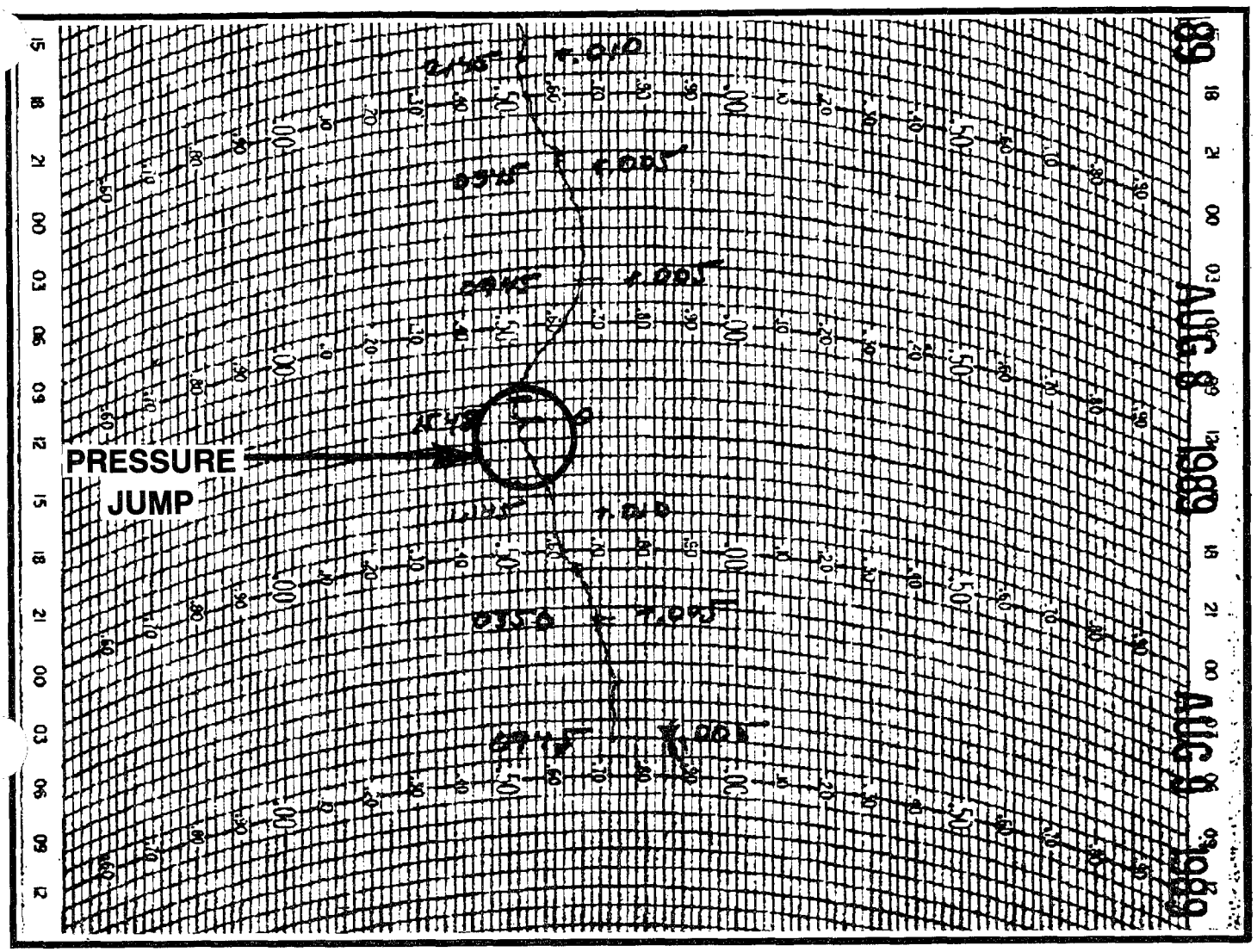

FIGURE 32
BARAGRAPH TRACE FROM WSO - LAS VEGAS

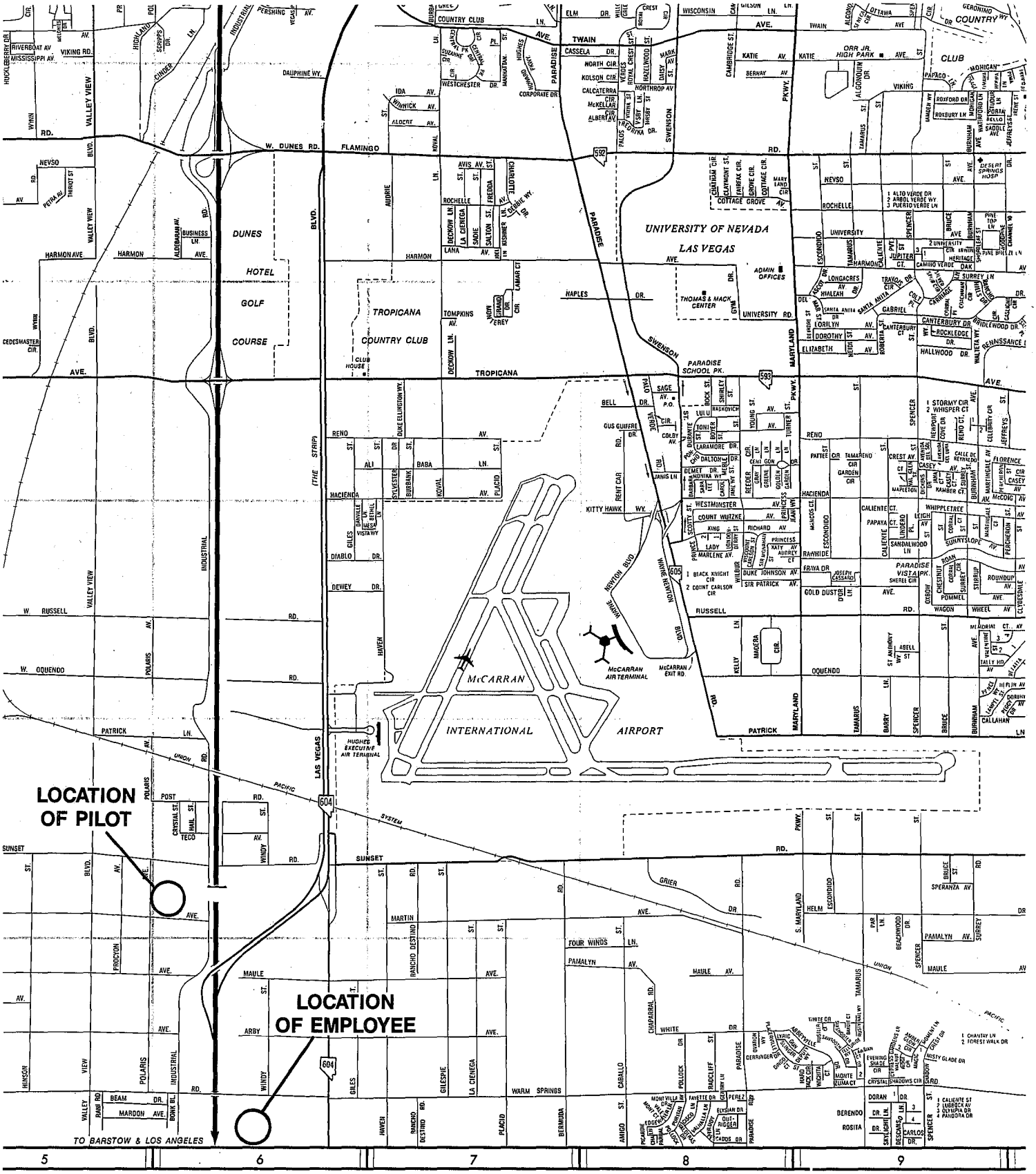

FIGURE 33
APPROXIMATE GROUND LOCATIONS
OF MICROBURST WITNESSES

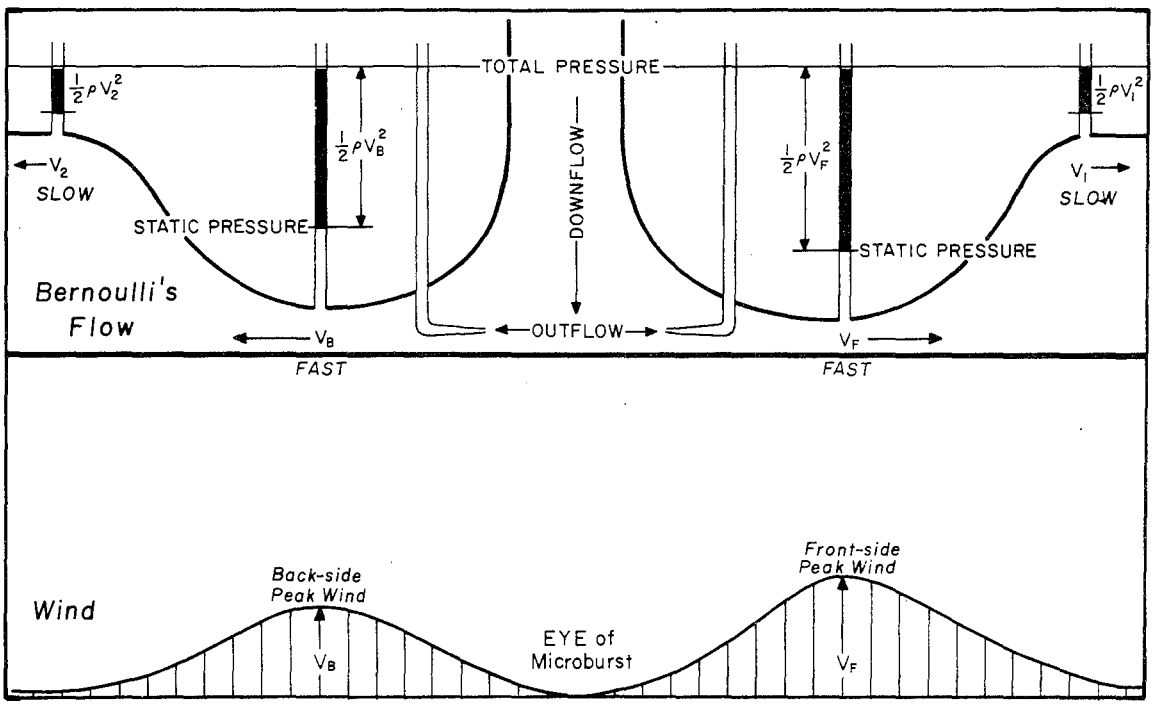

FIGURE 34
BERNOULLI'S THEOREM INDICATING THAT THE TOTAL PRESSURE, A SUM OF THE STATIC PRESSURE AND THE VELOCITY PRESSURE OR THE DYNAMIC PRESSURE, REMAINS CONSTANT DURING A FRICTIONLESS OUTFLOW FROM THE CENTER OF A MICROBURST. (FUJITA, 1985)

142 The Usefulness of Data from Mountaintop Fire Lookout Stations in Determining Atmospheric Stability. Jonathan W. Corey, April 1979. (PB298899/AS)
143 The Depth of the Marine Layer at San Diego as Related to Subsequent Cool Season Precipitation Episodes in Arizona. Ira S. Brenner, May 1979. (PB298817/AS)
144 Arizona Cool Season Climatological Surface Wind and Pressure Gradient Study. Ira S. Brenner, May 1979. (PB298900/AS)
146 The BART Experiment. Morris S. Webb, October 1979. (PB80 155112)
147 Occurrence and Distribution of Flash Floods in the Western Region. Thomas L. Dietrich, December 1979. (PB80 160344)
149 Misinterpretations of Precipitation Probability Forecasts. Allan H. Murphy, Sarah Lichtenstein, Baruch Fischhoff, and Robert L. Winkler, February 1980. (PB80 174576)
150 Annual Data and Verification Tabulation - Eastern and Central North Pacific Tropical Storms and Hurricanes 1979. Emil B. Gunther and Staff, EPHC, April 1980. (PB80 220486)
151 NMC Model Performance in the Northeast Pacific. James E. Overland, PMEL-ERL, April 1980. (PB80 196033)
152 Climate of Salt Lake City, Utah. Wilbur E. Figgins (Retired) and Alexander R. Smith. Fourth Revision, March 1989. (PB89 180624/AS)
153 An Automatic Lightning Detection System in Northern California. James E. Rea and Chris E. Fontana, June 1980. (PB80 225592)
154 Regression Equation for the Peak Wind Gust 6 to 12 Hours in Advance at Great Falls During Strong Downslope Wind Storms. Michael J. Oard, July 1980. (PB91 108367)
155 A Raininess Index for the Arizona Monsoon. John H. Ten Harkel, July 1980. (PB81 106494)
156 The Effects of Terrain Distribution on Summer Thunderstorm Activity at Reno, Nevada. Christopher Dean Hill, July 1980. (PB81 102501)
157 An Operational Evaluation of the Scofield/Oliver Technique for Estimating Precipitation Rates from Satellite Imagery. Richard Ochoa, August 1980. (PB81 108227)
158 Hydrology Practicum. Thomas Dietrich, September 1980. (PB81 134033)
159 Tropical Cyclone Effects on California. Arnold Court, October 1980. (PB81 133779)
160 Eastern North Pacific Tropical Cyclone Occurrences During Intraseasonal Periods. Preston W. Leftwich and Gail M. Brown, February 1981. (PB81 205494)
161 Solar Radiation as a Sole Source of Energy for Photovoltaics in Las Vegas, Nevada, for July and December. Darryl Randerson, April 1981. (PB81 224503)
162 A Systems Approach to Real-Time Runoff Analysis with a Deterministic Rainfall-Runoff Model. Robert J.C. Burnash and R. Larry Ferral, April 1981. (PB81 224495)
163 A Comparison of Two Methods for Forecasting Thunderstorms at Luke Air Force Base, Arizona. LTC Keith R. Cooley, April 1981. (PB81 225393)
164 An Objective Aid for Forecasting Afternoon Relative Humidity Along the Washington Cascade East Slopes. Robert S. Robinson, April 1981. (PB81 23078)
165 Annual Data and Verification Tabulation, Eastern North Pacific Tropical Storms and Hurricanes 1980. Emil B. Gunther and Staff, May 1981. (PB82 230336)
166 Preliminary Estimates of Wind Power Potential at the Nevada Test Site. Howard G. Booth, June 1981. (PB82 127036)
167 ARAP User's Guide. Mark Mathewson, July 1981, Revised September 1981. (PB82 196783)
168 Forecasting the Onset of Coastal Gales Off Washington-Oregon. John R. Zimmerman and William D. Burton, August 1981. (PB82 127051)
169 A Statistical-Dynamical Model for Prediction of Tropical Cyclone Motion in the Eastern North Pacific Ocean. Preston W. Leftwich, Jr., October 1981. (PB82195298)
170 An Enhanced Plotter for Surface Airways Observations. Andrew J. Spry and Jeffrey L. Anderson, October 1981. (PB82 153883)
171 Verification of 72-Hour 500-MB Map-Type Predictions. R.F. Quiring, November 1981. (PB82 158098)

172 Forecasting Heavy Snow at Wenatchee, Washington. James W. Holcomb, December 1981. (PB82 177783)
173 Central San Joaquin Valley Type Maps. Thomas R. Crossan, December 1981. (PB82 196064)
174 ARAP Test Results. Mark A. Mathewson, December 1981. (PB82 198103)
176 Approximations to the Peak Surface Wind Gusts from Desert Thunderstorms. Darryl Randerson, June 1982. (PB82 253089)
177 Climate of Phoenix, Arizona. Robert J. Schmidli, April 1969 (Revised December 1986). (PB87 142063/AS)
178 Annual Data and Verification Tabulation, Eastern North Pacific Tropical Storms and Hurricanes 1982. E.B. Gunther, June 1983. (PB85 106078)
179 Stratified Maximum Temperature Relationships Between Sixteen Zone Stations in Arizona and Respective Key Stations. Ira S. Brenner, June 1983. (PB83 249904)
180 Standard Hydrologic Exchange Format (SHEF) Version I. Phillip A. Pasteries, Vernon C. Bissel, David G. Bennett, August 1983. (PB85 106052)
181 Quantitative and Spacial Distribution of Winter Precipitation along Utah's Wasatch Front. Lawrence B. Dunn, August 1983. (PB85 106912)
182 500 Millibar Sign Frequency Teleconnection Charts - Winter. Lawrence B. Dunn, December 1983. (PB85 106276)
183 500 Millibar Sign Frequency Teleconnection Charts - Spring. Lawrence B. Dunn, January 1984. (PB85 111367)
184 Collection and Use of Lightning Strike Data in the Western U.S. During Summer 1983. Glenn Rasch and Mark Mathewson, February 1984. (PB85 110534)
185 500 Millibar Sign Frequency Teleconnection Charts - Summer. Lawrence B. Dunn, March 1984. (PB85 111359)
186 Annual Data and Verification Tabulation eastern North Pacific Tropical Storms and Hurricanes 1983. E.B. Gunther, March 1984. (PB85 109635)
187 500 Millibar Sign Frequency Teleconnection Charts - Fall. Lawrence B. Dunn, May 1984. (PB85 110930)
188 The Use and Interpretation of Isentropic Analyses. Jeffrey L. Anderson, October 1984. (PB85 132694)
189 Annual Data & Verification Tabulation Eastern North Pacific Tropical Storms and Hurricanes 1984. E.B. Gunther and R.L. Cross, April 1985. (PB85 1878887AS)
190 Great Salt Lake Effect Snowfall: Some Notes and An Example. David M. Carpenter, October 1985. (PB86 119153/AS)
191 Large Scale Patterns Associated with Major Freeze Episodes in the Agricultural Southwest. Ronald S. Hamilton and Glenn R. Lussky, December 1985. (PB86 144474AS)
192 NWR Voice Synthesis Project: Phase I. Glen W. Sampson, January 1986. (PB86 145604/AS)
193 The MCC - An Overview and Case Study on Its Impact in the Western United States. Glenn R. Lussky, March 1986. (PB86 170651/AS)
194 Annual Data and Verification Tabulation Eastern North Pacific Tropical Storms and Hurricanes 1985. E.B. Gunther and R.L. Cross, March 1986. (PB86 170941/AS)
195 Radid Interpretation Guidelines. Roger G. Pappas, March 1986. (PB86 177680/AS)
196 A Mesoscale Convective Complex Type Storm over the Desert Southwest. Darryl Randerson, April 1986. (PB86 190998/AS)
197 The Effects of Eastern North Pacific Tropical Cyclones on the Southwestern United States. Walter Smith, August 1986. (PB87 106258AS)
198 Preliminary Lightning Climatology Studies for Idaho. Christopher D. Hill, Carl J. Gorski, and Michael C. Conger, April 1987. (PB87 180196/AS)
199 Heavy Rains and Flooding in Montana: A Case for Slantwise Convection. Glenn R. Lussky, April 1987. (PB87 185229/AS)
200 Annual Data and Verification Tabulation Eastern North Pacific Tropical Storms and Hurricanes 1986. Roger L. Cross and Kenneth B. Mielke, September 1987. (PB88 110895/AS)
201 An Inexpensive Solution for the Mass Distribution of Satellite Images. Glen W. Sampson and George Clark, September 1987. (PB88 114038/AS)
202 Annual Data and Verification Tabulation Eastern North Pacific Tropical Storms and Hurricanes 1987. Roger L. Cross and Kenneth B. Mielke, September 1988. (PB88 101935/AS)
203 An Investigation of the 24 September 1986 "Cold Sector" Tornado Outbreak in Northern California. John P. Monteverdi and Scott A. Braun, October 1988. (PB89 121297/AS)
204 Preliminary Analysis of Cloud-To-Ground Lightning in the Vicinity of the Nevada Test Site. Carven Scott, November 1988. (PB89 128649/AS)
205 Forecast Guidelines For Fire Weather and Forecasters -- How Nighttime Humidity Affects Wildland Fuels. David W. Goens, February 1989. (PB89 162549/AS)
206 A Collection of Papers Related to Heavy Precipitation Forecasting. Western Region Headquarters, Scientific Services Division. August 1989. (PB89 230833/AS)

NOAA SCIENTIFIC AND TECHNICAL PUBLICATIONS

The National Oceanic and Atmospheric Administration was established as part of the Department of Commerce on October 3, 1970. The mission responsibilities of NOAA are to assess the socioeconomic impact of natural and technological changes in the environment and to monitor and predict the state of the solid Earth, the oceans and their living resources, the atmosphere, and the space environment of the Earth.

The major components of NOAA regularly produce various types of scientific and technical information in the following kinds of publications.

PROFESSIONAL PAPERS--Important definitive research results, major techniques, and special investigations.

CONTRACT AND GRANT REPORTS--Reports prepared by contractors or grantees under NOAA sponsorship.

ATLAS--Presentation of analyzed data generally in the form of maps showing distribution of rainfall, chemical and physical conditions of oceans and atmosphere, distribution of fishes and marine mammals, ionospheric conditions, etc.

TECHNICAL SERVICE PUBLICATIONS--Reports containing data, observations, instructions, etc. A partial listing includes data serials; prediction and outlook periodicals; technical manuals, training papers, planning reports, and information serials; and miscellaneous technical publications.

TECHNICAL REPORTS--Journal quality with extensive details, mathematical developments, or data listings.

TECHNICAL MEMORANDUMS--Reports of preliminary, partial, or negative research or technology results, interim instructions, and the like.

Information on availability of NOAA publications can be obtained from:

NATIONAL TECHNICAL INFORMATION SERVICE

U. S. DEPARTMENT OF COMMERCE

5285 PORT ROYAL ROAD

SPRINGFIELD, VA 22161